Automated Implementation and Validation of the Edinburgh Visual Gait Score (EVGS)

Ishaasamyuktha Somasundaram

Thesis submitted to the Faculty of Engineering
in partial fulfillment of requirements for the degree of

Master of Applied Science

in

Biomedical Engineering

uOttawa

Ottawa Carleton Institute for Biomedical Engineering
University of Ottawa
Ottawa, Ontario

Abstract

Gait analysis is an integral component of physical and neurological status assessment in humans. The Edinburgh Visual Gait Score (EVGS) is a reliable and clinically feasible scoring system for visual gait analysis. Clinical use of EVGS relies on manual scoring of video recordings, which is a point where automation can be utilized to gain even higher efficiency and accuracy.

In this thesis, an algorithmic implementation of EVGS scoring using patient videos was implemented and evaluated. Videos with EVGS manual scores were obtained from the Sanatorio del Norte medical center dataset, providing sagittal and coronal plane views of people with cerebral palsy walking. Body keypoints representing joints and limb segments were identified using the OpenPose Body 25 pose estimation model. The algorithm used these keypoints to identify foot events, strides, and relevant body angles, which were used by the algorithm to automatically score each EVGS parameter. The stride identification results were compared against the ground truth foot events and EVGS results were compared with expert scorer evaluations.

The algorithm was excellent for plane detection and movement direction classification, in both sagittal and coronal views. Stride detection was accurate for the majority of videos. Of the 17 EVGS parameters evaluated, six had an accuracy of 90-94%, five had a high accuracy of 84-89%, three a moderate accuracy of 70-76%, while the final three had a low accuracy of 58-62%. The results support use of the automated EVGS scoring approach to accelerate clinical visual gait analysis so that routine monitoring of patients can be performed without requiring extensive clinician time and enabling remote EVGS analysis at the point of patient contact.

Table of Contents

List of Figures

List of Tables

Abbreviations and Definitions

3D	Three Dimensional
AD	Alzheimer's disease
AI	Artificial Intelligence
CNN	Convolutional Neural Network
CP	Cerebral Palsy
EVGS	Edinburgh Visual Gait Score
G.A.I.T.	Gait Assessment and Intervention Tool
GMFCS	Gross Motor Function Classification System
ICC	Intraclass Correlation Coefficient
IGA	Instrumented Gait Analysis
MCID	Minimal Clinically Important Difference
MS	Multiple Sclerosis
OGA	Observational Gait Analysis
PD	Parkinson's disease
POMA	Performance-Oriented Mobility Assessment
PRS	Physician’s Rating Scale
PRS-OGS	PRS-Based Observational Gait Scale
ROC	Receiver-Operating Characteristic Curve
RVGA	Rivermead Visual Gait Assessment
SF-GT	Salford Gait Tool
SMS	Stroke Mobility Score
TDP	Time-Distance Parameters
TGS	Tinetti Gait Scale
VGA	Visual Gait Analysis
WGS	Wisconsin Gait Scale

Acknowledgments

I sincerely thank and appreciate my supervisors, Prof. Natalie Baddour and Prof. Edward Lemaire, for their unwavering support and guidance throughout my research journey. Their belief in me and the opportunity to work at the Mobile Motion Lab were instrumental in the completion of this thesis. Their weekly support, even during slow progress periods, along with their informative guidance and patience, were invaluable. They not only assisted me in becoming more organized but also taught me to think like a researcher when approaching problems.

I extend my heartfelt gratitude to Dr. Albert Tu and Dr. Kevin Cheung from CHEO, whose vast clinical knowledge and expertise in EVGS were crucial to this research. Their continuous assistance and contributions were indispensable to the success of this project.

My deepest appreciation goes to my family, especially my mother, Yamuna Somasundaram. Her unwavering support, guidance, and unconditional love have been a constant source of inspiration, motivating me to express myself more clearly and achieve all my goals. I am forever indebted to her for her countless sacrifices and ongoing support.

I would like to dedicate this thesis to the memory of my late grandfather, Sankaran. His unwavering support throughout my academic journey and his encouragement to pursue higher education were pivotal in driving me to complete this thesis, despite the challenges faced. His belief in my abilities and his support for my career goals will always be remembered and cherished.

Lastly, I extend my sincere thanks to all my friends and colleagues at The University of Ottawa, Ottawa Hospital Rehabilitation Centre, The Children's Hospital of Eastern Ontario and doctors of Sanatorio del Norte for their invaluable assistance with data collection and validation. Your support and collaboration have significantly contributed to the success of this research.

1 Introduction

Gait, defined as the pattern of walking or running, is a fundamental aspect of human movement characterized by a complex interplay of muscles, joints, and neurological pathways [1]. Gait analysis, the systematic observation of human locomotion, is an important tool in medical diagnostics and rehabilitation because such analysis gives important insight into a person's health condition and movement status. Gait assessments are reported for people with neurological disorders such as Parkinson's disease (PD), Multiple Sclerosis (MS), and Alzheimer's disease (AD) to identify gait disturbances such as reduced stride length, freezing of gait, and increased variability [2], [3], [4]. In the case of MS, gait disturbances, such as leg paresis and spasticity, may become apparent very early, often before the time of visible manifestation. Similarly, reduced gait speed and increased variability among AD patients have underlined gait as an early biomarker for neurodegenerative diseases [5], [6].

Gait can be clinically assessed using timed tests like the 10-meter walking test or laboratory-based systems that include motion capture and force plates. Laboratory methods provide detailed biomechanical data, but are costly, require expert personnel, and take extensive time for data collection, processing, and analysis. Observational scales have been used to provide some standardization of visual assessment of gait patterns in the clinical setting [7], [8]. Various visual gait assessment tools [9], [10] and scales have been developed to assess the neurological conditions that most affect gait, such as PD, MS, Cerebral Palsy (CP), and stroke. Of these, the Gait Assessment Intervention Tool (G.A.I.T.) is one of the most elaborate scales designed to assess gait disturbances in neurological patients. The Rivermead Visual Gait Assessment is another commonly used tool for the analysis of gait in neurological patients [11]. The Wisconsin Gait Scale was developed to especially investigate gait in survivors of a stroke [12]. Further, the Edinburgh Visual Gait Score, which has long been used to investigate children with CP, also applies to a wider number of neurological uses. In as much as these instruments are all different from one another in various ways concerning their reliability and validity, each nevertheless has gained substantially in practice in normalizing visual gait abnormality assessment [8]

Pose estimation is a computer vision algorithm for estimating and locating a human's joints or keypoints in an image or a video [13] [14], generating a human skeletal model for a range of applications, such as gaming, medical, augmented reality, and sports analysis [13], [15]. This markerless approach could provide a less costly alternative to conventional motion capture technology[16], with potential for extending access to gait analysis by enabling video-based data collection at any location using minimal equipment.

Recent video-based pose estimation algorithm developments have enabled the application of digital video to analyze human motion [17], [18], [19], [20]. These algorithms use digital videos that could be captured from everyday devices, including smartphones, to identify 2D coordinates of body joints and other landmarks. These keypoints can be used to calculate spatiotemporal parameters such as step length, step time, and joint kinematics. The accuracy of video-based methodologies can be very high, with evidence of direct comparisons with the gold standard of motion capture systems. For example, sagittal video recordings can provide accurate gait kinematics of the hip and knee during overground or treadmill walking in patients with stroke [21]. Video of a person walking can be captured outside of the lab-environment to home or clinics, which may be very useful for continuous monitoring. Pose estimation-based methods could be applied to create an automated clinical video scoring system that would enhance accessibility of quantitative movement analysis, minimize expert time, and reduce the need for specialized equipment.

1.1 Rationale

Gait analysis is a useful tool for assessing mobility status and neurological effects on movement and is usually conducted in 3D instrumented gait laboratories. However, not all patients can access such facilities. In children with mobility impairments, such as those with CP, the logistic challenges in attending a motion analysis lab are exacerbated by the needs of the parents to arrange additional care, to take time off work, and to risk hazardous traveling conditions in winter months. These make frequent gait analyses impracticable and inhibit the possibility of timely monitoring and intervention.

A video approach could provide a flexible and inexpensive method to record high-quality footage of the patient’s movements in clinical or nonclinical environments. With recent advances in AI, pose estimation algorithms can identify a person’s joint locations to enable gait parameter

calculations and reporting. This approach could help make gait analysis more available, especially to rural or otherwise underserved communities without access to a typical gait lab.

Of the many instruments developed for visual gait analysis, Edinburgh Visual Gait Score (EVGS) is a reliable tool for assessing walking, especially in children with cerebral palsy. A clinician visually rates a patient's videos for the purpose of tracking changes and intervention outcomes. However, EVGS scoring requires considerable time and labor from a human rater, with every evaluation taking an average of 24.7 minutes [22]. An automated approach for scoring EVGS would remove the time barriers for implementing this tool in daily practice.

Patient videos are not always captured under optimal conditions, often presenting with undesirable features such as zooming in and out, parts of the person outside the video frame, or assistants walking with the patient adversely affecting pose estimation. These conditions are problematic for automated gait analysis via videos, which became apparent when initially applying the previous algorithm by Ramesh et al. [23] to a clinical dataset. Automation algorithms would need specific functions to deal with these, and other, issues before generating an acceptable EVGS score.

This thesis addresses these needs by developing and evaluating an automated system for EVGS scoring clinical videos of people with CP. A successful system could make EVGS analysis more accessible by improving analysis speed, reducing reliance on specialized equipment, and avoiding subjective manual grading to eventually improve clinical decision-making.

1.2 Scope

This research focuses on people with CP that require visual gait analysis using EVGS. Since EVGS ranges and values were adapted for the CP population, the parameters of the study are limited to the same category of patients. However, the automated EVGS system could be easily extended to other populations using different, validated video-based gait assessment scales. The Sanatorio del Norte medical center dataset, used in this research, contains clinical video from participants in Argentina; hence, generalization beyond this dataset cannot be confirmed without further research.

1.3 Objectives

The goal of this research is to implement and evaluate an automated system for EVGS scoring of videos taken of CP patients in a clinical environment. This thesis presents the first

implementation of an automated EVGS scoring system with CP patients in a clinical environment. Specific objectives are

- Objective 1: Develop an algorithm to detect plane of motion capture, strides, direction of movement and automatically determine the EVGS score from sagittal and coronal view patient videos.
- Objective 2: Validate the algorithm on a large clinical dataset

1.4 Thesis Contributions

This thesis resulted in a viable EVGS scoring system that can automatically calculate EVGS parameter scores from clinical videos. The following contributions were made to the automated gait analysis field:

1. An automated scoring system was developed and tested that successfully identified the plane of motion capture, direction of movement and strides, and then automatically scored the EVGS from video recordings.

2. Developed a novel plane detection algorithm that detects the two important anatomical planes, sagittal and coronal, which are essential for proper EVGS scoring. The new method solves issues when applying the original Ramesh et. al. [23] algorithm to the clinical dataset.

3. Designed a versatile algorithm capable of detecting patient movement direction in sagittal and coronal planes, applicable not only to EVGS but also to other visual gait analysis indices and biomechanical analyses using markerless motion capture.

4. Demonstrated system validity with patient videos from a clinical facility. Previously, a purpose-built dataset of able-bodied individuals performing movements that covered the full range of EVGS scores was used to validate the automated scoring algorithm. This thesis identified and resolved problems when applying the original algorithms to typical clinical videos, making the new EVGS scoring system more robust.

5. The system is optimized for speed and could provide an EVGS report in less than 60 seconds for a 10-15 second patient video. This short turnaround time enables clinicians to interpret the results at the point of patient contact. If needed, additional videos could be taken and reanalyzed

during the same appointment, eliminating the need for patients to book repeat appointments or return to the clinic. This efficient use of time and clinical resources could improve patient experience and workflow for clinicians. Automated calculation of EVGS will lower the burden on clinicians since computations will be automated, without any involvement from the clinicians.

1.5 Thesis Outline

Chapter 2 provides a literature review covering gait biomechanics, current gait analysis methods, various observational gait assessment scales, and deep learning models for human pose estimation.

Chapter 3 presents a comparative analysis of previous and improved methods for automating EVGS scoring system.

Chapter 4 describes the development and evaluation of the proposed automated EVGS scoring system.

Chapter 5 describes the validation of the proposed system with a large clinical database of CP patient that have been manually EVGS scored by experts.

Chapter 6 summarizes the thesis, main results, and further directions of study.

2 Literature Review

2.1 Gait

Gait is the manner of walking or running and is a complex process that involves the interaction of various systems in the human body [24]. The gait cycle has been divided into stance and swing phases, periods, and events [25] (Figure 2.1). A gait cycle starts with a foot strike and concludes with a foot strike on the same side of the body. The events involved in a normal gait cycle include foot strike and foot off on each leg. Periods include loading response, mid-stance, terminal stance, pre-swing, mid-swing, and terminal swing. Every gait cycle is further divided into stance and swing phases. The stance phase ranges from foot strike to toe-off, and the swing phase commences with a toe-off and ends with a foot strike [26].

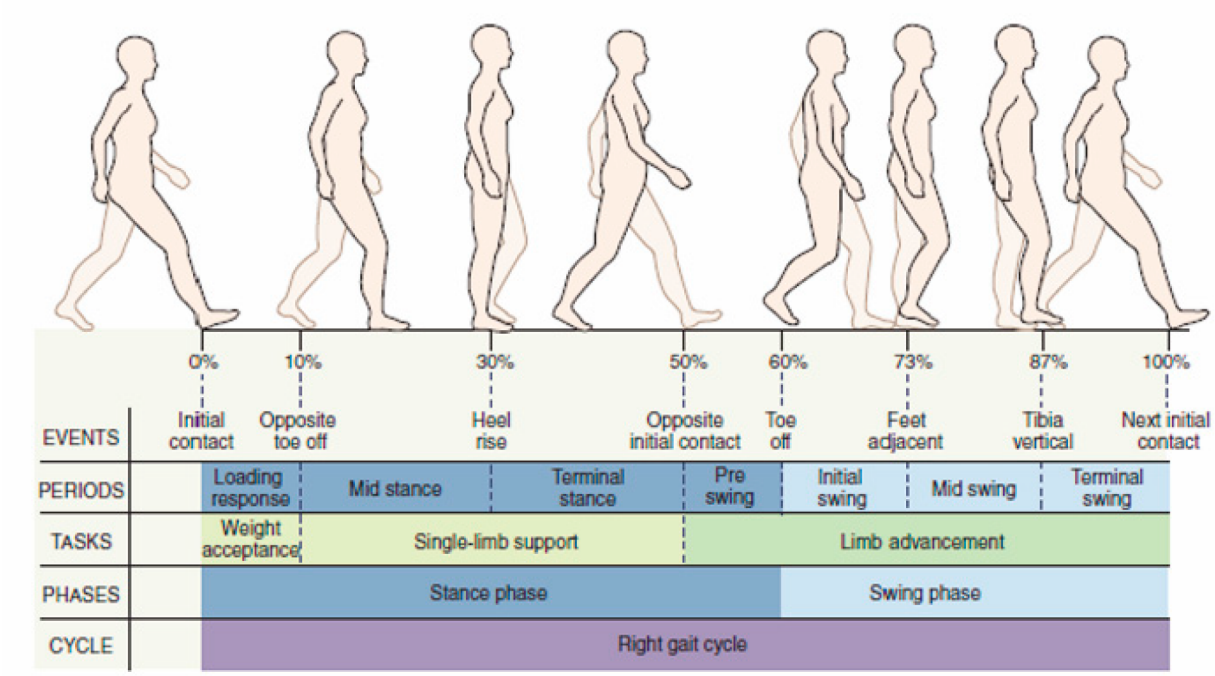

Figure 2.1 Gait cycle [27]

Various stride parameters are utilized in clinical quantitative gait analysis [1]:

- **Stride length:** linear distance of successive points of initial contact of the same foot.
- **Step length:** linear distance of one foot from the point of initial contact to the point of initial contact of the opposite foot.
- **Walking speed (gait velocity):** time to walk a certain distance

- **Cadence:** number of steps taken per minute
- **Stride time:** time from initial contact of one foot to the subsequent initial contact of the same foot
- **Step width:** medial-lateral distance between the heels of the two feet when they first make contact with the ground

2.1.1 Stance Phase

Stance phase accounts for 60% of the entire gait cycle and is defined as the period when the foot is in contact with the ground. Stance is divided into five sub- phases [28], [29], [30]:

- **Initial contact or heel strike:** This is the initial contact of the foot with the ground and marks the commencement of stance phase. During this time, the ankle is usually in a neutral position, the knee slightly flexed, and the hip flexed to about 30 degrees [31], [32].
- **Loading response:** After initial contact, the foot dorsiflexes until the whole plantar surface touches the floor. The weight of the body is absorbed, and weight transfer to the supporting foot occurs [33], [34].
- **Mid-stance:** Body centre of gravity passes directly over the supporting foot. The knee and hip extend, and the contralateral limb swings forward [35].
- **Terminal stance:** As the body continues to move forward, the heel comes off the ground. Hip and knee extension increases. At terminal stance single-limb support, the ankle is at maximal dorsiflexion of 10°, then reverses to 5° of plantar flexion [36]. The hip extends and reaches 10° hyperextension, whereby the knee extends to its maximum range of 0 to -5° [9].
- **Pre-swing:** This is the final event of the stance phase, marked by rapid hip extension and the onset of knee flexion [35].

In stance phase, the muscles around the lower limb act in concert in controlling joint movements and also perform shock absorption. For example, during initial contact, the quadriceps muscles are contracting eccentrically to control knee flexion, while the gastrocnemius and soleus muscles make very important contributions during terminal stance and pre-swing. In early stance, the quadriceps muscles are the primary contributors to braking and support, while the soleus and gastrocnemius

muscles contribute significantly to propulsion and support in late stance [37]. The gastrocnemius and quadriceps muscles exhibit co-activation patterns throughout the gait cycle, which may affect knee joint stability and ligament strain [38].

Individual muscle contributions to joint contact forces vary similarly: vastii muscles are believed to contribute most to axial knee joint force in early stance whereas gastrocnemius is activated during late stance [39]. Muscles that do not directly cross the knee joint, such as the gluteus maximus and soleus, also contribute to knee joint forces indirectly through their effects on ground reaction forces. Indeed, references [39], [40] have reported that understanding such muscle contributions forms a basis for both prevention of joint injury and treatment of gait pathologies.

2.1.2 Swing Phase

Swing phase is the 40% of the gait cycle where the foot does not touch the ground, divided into initial swing, mid-swing, and terminal swing [18], [28], [41].

- **Initial swing:** This sub-phase begins at toe-off. The hip, knee, and ankle all flex to initiate the advance of the limb and also to give foot clearance over the ground. The main active muscles are the hip flexors, most especially the iliopsoas [35].
- **Mid-swing:** The thigh is now in the peak advancement as the limb is passing directly under the body. Knee flexion peaks around 60 degrees. Contraction of the tibialis anterior muscle maintains good ankle dorsiflexion, thus giving good foot clearance [35].
- **Terminal swing:** This is the last sub-phase where preparation for the next heel strike takes place. The knee starts extending, and the ankle remains in dorsiflexion. Hamstrings are activated to decelerate the swinging limb and control knee extension [35].

Swing phase advances the limb in preparation for the next step and involves accurate control of the hip, knee, and ankle to allow appropriate foot clearance and positioning before the next heel strike.

2.1.3 Double Support Periods

Double support occur at the beginning and end of stance phase, when both feet are in contact with the floor simultaneously, occupying approximately 20% of the gait cycle [42]. In both periods of double support, stability is achieved and a smooth transfer of weight between the limbs can occur.

2.1.4 Biomechanical Considerations

Walking is a complex interaction of various joints and muscle groups. The lower limb acts as a closed kinetic chain during stance phase, where the foot is fixed on the ground. Coordinated action of the ankle, knee, and hip joints against each other maintain stability and progress the body forward [43], [44]. By contrast, the lower limb becomes an open kinetic chain during the swing phase with much more range of motion [45]. Accurate muscle function is highly critical during this phase to ensure appropriate advancement of the limb and avoid an inappropriate foot strike.

2.2 Observational Gait Analysis

Gait analysis has been defined as the systematic study of human movement, including identifying and measuring body segment trajectories as a function of time [31], [46]. By analyzing gait, clinicians can diagnose gait abnormalities, detect balance factors, check the success of therapeutic treatments or surgical procedures, and make necessary therapeutic interventions. Instrumented gait analysis (IGA) is the gold standard in gait analysis [47] and requires hardware such as force plates, reflective markers attached to participants, inertial measurement units, or pressure measurement systems to gather quantitative information for kinematic, kinetic, or muscle activation analysis [32], [48]. IGA is a resource-intensive process, consuming a large amount of time, money, space, and personnel. Motion analysis laboratories are not available in most clinical settings.

To overcome these difficulties, observational gait analysis or visual gait analysis (VGA) provides a means whereby clinicians can observe and describe gait. VGA techniques are used to assess gait disorders both in adults and children [11], [46], [49], [50], [51], [52], where scorers view video recordings and rate the recorded gait using various scales, each one evaluating specific joints, planes, and gait cycle events. Several computer-assisted image analysis techniques have been developed to aid clinicians, allowing joint angle measurement and recording other movements and postures. This approach, because it is simpler and more accessible than IGA, is preferred by many clinicians, or sometimes the only option available [53]. However, VGA is highly subjective and potentially can provide low sensitivity, specificity, validity, and reliability when compared with methods like the IGA. Despite all these potential shortcomings, clinicians continue to use VGA and depend on it in clinical settings [54].

2.3 Types of Visual Gait Analysis

2.3.1 Physician's Rating Scale (PRS)

Among the first modern observational indices for gait analysis, the Physician's Rating Scale was developed in 1993 to evaluate cerebral palsy in children by using walking sequences on video [55]. PRS examines six parameters for each leg, including gait speed and kinematics related to the hip, knee, ankle, and foot. In this scale, clinicians visually rate and then manually score gait deviations based on a multi-point ordinal scale Table 2.1. The summary score allows clinicians to assess changes between interventions (e.g., pre- and post-surgery).

Despite such scope and simplicity, PRS has attracted a considerable amount of criticism. The failure to standardize different scoring methodologies resulted in inter-rater reliability issues. Different clinicians often score the same patient differently [8], [56]. Modifications were proposed to enhance reliability and sensitivity, although most revisions produced mixed results. Despite these drawbacks, PRS laid the groundwork for more refined observational indices by providing a fundamental framework for scoring and analysis of gait abnormalities [49], [57], [58].

2.3.1 PRS-Based Observational Gait Scale (PRS-OGS)

The PRS-Based Observational Gait Scale (PRS-OGS) is the modification of the original PRS, and was developed to assess children with CP, scoring eight parameters: knee, ankle, foot progression, and the use of assistive devices [59]. PRS scoring was modified and became even more responsive to therapeutic changes following some interventions, like botulinum toxin treatments [59], [60].

Table 2.1 Visual Gait Assesment Scale - adapted from PRS [61]

Parameter	Category		Score
Hip in terminal stance	Hyperflexed Mod-mild flexion Normal (extended)	> 20° 0° - 20° <0°	1 2 3
Hip in mid swing	Hyperflexed Decreased flexion Normal (extended)	>45° < 25° 25°-45°	1 2 3
Knee peak extension in terminal stance	Flexion – severe Flexion - mild Normal Recurvatum	> 30° 16° - 30° 0° - 15° <0°	1 2 3 4
Knee peak flexion in swing	Hyperflexed Decreased flexion Normal (extended)	>70° < 50 50°-70°	1 2 3
Initial foot contact	Forefoot Foot flat Heel		1 2 3
Foot contact in stance	Toe / toe (equinus) Foot flat / early heel rise Foot flat / no early heel rise Occasional heel / foot flat Heel / toe (normal roll-over)		1 2 3 4 5
Timing of heel rise	No heel contact (equinus) Pre swing / stance limb level Just after swing / stance limb level Just pre – double support (normal) After double support (delayed)		1 2 3 4 5

PRS-OGS is focused on providing interventions such as botulinum toxin therapy by monitoring changes in gait patterns. PRS-OGS provided acceptable inter- and intra-rater reliability in most knee and foot aspects [60], but PRS-OGS has poor reliability for base of support and hindfoot position [60]. Similarly, biomechanical measurements of the lower extremities exhibited low interrater reliability, except for relaxed calcaneal stance position and forefoot varus, while intrarater reliability is generally high [62]. Visual assessment of postural orientation, particularly knee-medial-to-foot position, was reliable within and between raters and valid when compared with 2D and 3D kinematics in asymptomatic populations [63]. However, other segment-specific postural orientation errors demonstrated poor to moderate reliability or lack sufficient studies for conclusive evaluation [63]. Static biomechanical assessments of the foot and lower limb, commonly used in clinical practice, generally demonstrate poor inter-assessor reliability [64].

2.3.2 Wisconsin Gait Scale

The Wisconsin Gait Scale (WGS) was designed for hemiplegic stroke patients and consists of 14 items concerning trunk, pelvis, and lower limb kinematics, walking strategies, and the use of assistive devices [65].In contrast to previous indices, the WGS uses a weighted ordinal scale, focusing mainly on the affected leg. WGS is very sensitive to detecting changes, such as that occurring after gait training programs. Several studies demonstrated excellent internal consistency, high interrater reliability (ICC 0.83-0.96), and good intrarater reliability (ICC 0.75-0.96) [66], [67], [68], [69]. In addition, the scale demonstrated significant correlations with relevant clinical measures such as walking speed and Fugl-Meyer assessment [68]. However, several items, including "hip hiking at mid-swing," "circumduction at mid-swing," and "hip extension of the affected leg," had low reliability [69]. Despite several limitations, WGS represents a promising tool for making observational gait analysis more objective and more reliable in clinical practice, not needing much training to be effectively applied [66], [67].

2.3.3 Rivermead Visual Gait Assessment

The Rivermead Visual Gait Assessment (RVGA) grades 20 kinematic features of the upper limbs, trunk, and lower limbs in stance and swing phases using a four-point ordinal scale and was designed for patients with neurological disorders [11], [12], [70]. RVGA development was based on evidence that an experienced physical therapist can make accurate and reliable judgments of the kinematic aspects of movement with observational assessment [71]. This low-cost tool is especially useful in developing countries where gait analysis equipment is usually quite expensive [70]. The RVGA demonstrated good-excellent inter-rater reliability and test-retest reliability with acceptable validity when compared to other mobility measures [70].

2.3.4 Observational Gait Analysis

Observational Gait Analysis (OGA) index (Table 2.2) was designed for spastic diplegic CP patients older than eight years. Ten gait events are evaluated for ankle, knee, and hip, and pelvis kinematics in three anatomical planes [46]. OGA demonstrated moderate to good validity and reliability for temporo-spatial parameters [72]. Accuracy fluctuates with kinematic parameters: knee flexion and pelvic tilt showed higher validity compared to other planes and angles of movement [72], [73].

Moderate to good inter-rater reliability was observed, since about two-thirds of the observations demonstrated total agreement between raters [52]. Enhancing OGA through mobile technology demonstrated good reliability between raters on most measures but the authors advised caution in terms of transverse plane deviation quantification [74]. While providing a useful framework in guiding systematic gait assessment, particularly within the pediatric population, the accuracy and reliability of the OGA have room for further development in comparison with three dimensional gait analysis [73], [74].

Table 2.2 Observational Gait Analysis checklist [75]

	STANCE			SWING			
	LR	MSI	TSt	PSw	ISw	MSw	TSw
Trunk							
forward lean							
backward lean							
lateral lean (R/L)							
Pelvis							
no forward rotation (R/L)							
no contralateral drop (R/L)							
hiking (R/L)							
Hip							
inadequate extension							
circumduction/abduction							
Knee							
excessive flexion							
uncontrolled extension							
inadequate flexion							
Ankle/Foot							
foot slap							
forefoot contact							
foot flat contact							
late heel off							
contralateral vaulting							

2.3.5 Salford Gait Tool

Salford Gait Tool (SF-GT) was designed evaluate hip, knee, and ankle joint angles at six different

gait events (Figure 2.2), using a five-point scale [76]. The strength of SF-GT is that its results have been iteratively refined toward correspondence with quantitative kinematic data, which optimizes its reliability and clinical utility [77]. Since a limited number of gait parameters are analyzed, SF-GT may not be as comprehensive as other tools such as the EVGS.

APPENDIX 1: SALFORD GAIT TOOL—SAGITTAL (SIDE) PLANE VIEW

Enter the observed degrees of ranges of movement in the spaces below. Then assign a CATEGORY from the list on the left for each joint.

Name: Date: Diagnosis:	Initial Contact		End Double Support		Mid Stance		Start Double Support		Toe off		Mid Swing		Sum of Category Scores
													
TRUNK Circle observation:	normal backwards forwards		normal backwards forwards		normal backwards forwards		normal backwards forwards		normal backwards forwards		normal backwards forwards		Overall: normal backwards forwards
HIP													(1)*
CATEGORY: −2=−21° or more extension −1=−6° to−20° extension 0=−5° ext to 15° flexion 1=16° to 45° flexion 2=46° or more flexion	degrees	category	degrees	category	degrees	category	degrees	category	degrees	category	degrees	category	
KNEE													(5)*
CATEGORY: −2=−16° or more extension −1=−6° to −15° extension 0=−5° ext to 10° flexion 1=11° to 45° flexion 2=46° or more flexion	degrees	category	degrees	category	degrees	category	degrees	category	degrees	category	degrees	category	
ANKLE													(0)*
CATEGORY: 2=21° or more DF 1=1° to 20° DF 0=neutral 0° to −15° PF −1=−16° to −45° PF −2=46° or more PF	degrees DF PF	category	degrees DF PF	category	degrees DF PF	category	degrees DF PF	category	degrees DF PF	category	degrees DF PF	category	
Ankle	toe strike flat foot heel strike				Heel off the floor? Yes No								

Figure 2.2 Salford Gait Assesment [70]

2.3.6 Gait Assessment and Intervention Tool

G.A.I.T. is an observational gait analysis tool that is mainly applied to patients undergoing rehabilitation after a stroke [9]. G.A.I.T. employs an extended ordinal scale, rating 31 gait parameters under: upper limb and trunk kinematics in the stance and swing phases, lower limb kinematics in the stance phase, and lower limb kinematics in the swing phase. Each parameter is rated upon a 0-3 scale, with higher scores for movement deviation away from normal.

G.A.I.T. was validated for use in stroke and multiple sclerosis patients, and translated into multiple languages [78]. Sensitivity was better than the Tinetti Gait Scale for detecting improvements

following gait training interventions [79]. G.A.I.T. can effectively capture incremental changes in gait components, making this tool valuable for tracking progress in rehabilitation settings [9]. G.A.I.T. exhibited strong intra- and inter-rater reliability, as well as the capacity to differentiate between various gait training interventions (pre/post treatment and between the treatment groups) [9]. When comparing the sensitivity of G.A.I.T. and Performance-Oriented Mobility Assessment (POMA) to assess recovery of stroke patients who underwent gait rehabilitation programs [79], G.A.I.T. was more sensitive to performance changes, detecting improvement in 91% of the analyzed participants. POMA detected only 59%. G.A.I.T. was able to identify alterations on the most advanced stages of the training program [79].

2.3.7 Stroke Mobility Score

The Stroke Mobility Score (SMS) addresses many of the shortcomings in the assessment of post-stroke gait, evaluating six non-redundant parameters that are representative of trunk posture, limb movements, and gait speed, using a four-point scale. SMS has high inter-rater reliability and also shows strong correlation with functional scales such as the 10-Meter Walk Test [80]. This tool performs very well in stroke-specific applications but has limited use in other pathologies because of its narrow scope.

2.3.8 Edinburgh Visual Gait Score

Developed to assess children with CP, the Edinburgh Visual Gait Score (EVGS) [50] scores 17 parameters (trunk, pelvis, hip, knee, ankle, and heel in the coronal, sagittal, and transverse planes) as normal, moderate, or severe. Two video views are required to implement the test: sagittal and coronal. Each EVGS parameter is scored on a 3-point ordinal scale: 0 indicates normal gait (within ±1.5 standard deviations of the mean); 1, moderate deviations (1.5 to 4.5 standard deviations from the mean), and 2, significant or severe deviations (more than 4.5 standard deviations from the mean) [50]. A low total score reflects fewer gait deviations. To facilitate a clear understanding and to ensure consistency in scoring, the 17 EVGS parameters were grouped according to foot events and gait cycle phases (Table 2.3). The EVGS scoring methods are detailed in [81]. Robinson et al. [82] determined the minimal clinically important difference (MCID) of EVGS to be 2.4, which corresponds with assessment tools based on functional observation (e.g., Gross Motor Function Classification System). These results confirm the utility of VGA, and particularly EVGS, for the

diagnosis and quantification of gait irregularities in CP patients.

Table 2.3 EVGS parameters [23]

	Foot events and gait phases	**EVGS parameters**
Sagittal	Initial contact/Terminal swing	Peak hip flexion in swing
		Knee extension in terminal swing
		Initial contact
	Midstance	Peak sagittal trunk position
		Pelvic rotation in midstance
		Heel lift
	Terminal stance	Peak hip extension in stance
		Peak knee extension in stance
		Max ankle dorsiflexion in stance
	Midswing	Peak knee flexion in swing
		Maximum ankle dorsiflexion in swing
		Foot clearance in swing
Coronal	Midstance	Maximum lateral shift of trunk
		Maximum pelvic obliquity in stance
		Knee progression angle
		Foot rotation
		Hindfoot valgus/varus

Ong et al. [83] assessed the intra-observer reliability of EVGS scoring among experienced and inexperienced raters by training six medical students to perform EVGS assessments. The study reported a mean Coefficient of Repeatability (CoR) of 5.15 for inexperienced observers and 4.21 for experienced observers, indicating that repeated observations by the same individual would typically vary by no more than approximately five points for inexperienced raters and slightly less for experienced ones. The CoR reflects the range within which 95% of differences between two repeated measures by the same observer are expected to fall. A lower CoR value signifies higher intra-observer reliability.

However, reliability improved with practice and for higher-functioning patients [84]. When compared to 3D gait analysis (3DGA), EVGS demonstrated moderate agreement, with experienced raters achieving higher accuracy [83], [84]. Clinical experience did improve the results [84], which likely means that reliability can be improved with training and better understanding of gait [85].

EVGS has high concurrent validity (i.e., the extent to which EVGS scores agree with those from other established gait assessment tools when measured at the same time) with good consistency with other assessment tools [86], [87]. The balance of depth with ease-of-use eventually made the EVGS a widely accepted tool in pediatric gait analysis.

2.4 Comparison of Visual Gait Analysis Tools

VGA includes a wide range of tools. Table 2.4 outlines the main features of each index in relation to their merits and areas of improvement [88].

While the Wisconsin Gait Scale and the Stroke Mobility Score deal with specific pathologies like hemiplegia or stroke [89], [90], others like the RVGA and G.A.I.T. are more generalized measures of neurological gait disorders [9], [11], [66], [67], [69]. This specificity is at an asset and a limitation. For instance, WGS has proven useful for hemiplegia and stroke conditions; however, its few items make its application limited in more other neurological conditions. More general tools, like the RVGA and G.A.I.T., are more adaptable but at the expense of loss of relevance to certain populations [9], [79], [91].

The types of scoring systems vary between tools. Measures with less categories, such as three-point scales, exhibit heightened reliability but may be less responsive to subtle changes in gait patterns. In contrast, where more categories are utilized, such as the five-point scale utilized in the Salford Gait Tool (SF-GT), there is heightened differentiation but inter-rater reliability may be sacrificed [92]. Generally, this may be a fair trade-off between reliability and responsiveness in the development and choice of observational gait indices.

The RVGA utilizes a four-point ordinal scale but has received criticism regarding the subjective nature of scoring, since explicit guidelines on rating the degree of deviation were not provided [11]. Thus, such subjective assessment may lead to inconsistent scores between raters.

G.A.I.T was developed with more objective guidelines, which might have improved its intra- and inter-rater reliability scores [9].

Table 2.4 Overview of visual gait analysis

	Target Population	Features	Strengths	Limitations
Physician's Rating Scale (PRS)	Pediatric population with CP	6 kinematic features per leg, including hip, knee, ankle, and foot	Earliest visual gait analysis, simple scoring system	Lack of standardization, poor inter-rater reliability, limited applicability beyond CP
PRS-Based Observational Gait Scale (PRS-OGS)	Pediatric population with CP	8 parameters: knee, ankle, foot progression, assistive device usage	Improved sensitivity to therapy (e.g., botulinum toxin treatment), better structured than PRS	Poor reliability for base of support and hindfoot position, limited to young children
Wisconsin Gait Scale (WGS)	Hemiplegic patients (post-stroke)	14 items focusing on trunk, pelvis, lower limbs, and walking strategies	Sensitive to post-therapy changes, fair correlation with time-distance parameters (TDP), strong for hemiplegic gait analysis	Low reliability for specific items (e.g., hip extension, foot circumduction)
Rivermead Visual Gait Assessment (RVGA)	Adults with neurological disorders	20 kinematic features of upper limbs, trunk, and lower limbs	Good reliability, correlations with walking time and stride length, sensitive to changes in gait performance	Exclusion of some key parameters limits use in musculoskeletal conditions
Edinburgh Visual Gait Score (EVGS)	Pediatric population with CP	17 parameters across sagittal, coronal, and transverse planes	High reliability and validity, comprehensive evaluation, strong correlation with functional scales	Primarily validated for pediatric CP; broader population studies needed
Observational Gait Analysis (OGA)	People with spastic diplegic CP	10 gait events in three anatomical planes	High inter-rater reliability	Limited agreement with 3D kinematic data, restricted to specific parameters
Salford Gait Tool (SF-GT)	Pediatric population with CP	Hip, knee, and ankle angles across 6 distinct gait events	Alignment with quantitative data, relatively reliable	Limited scope compared to EVGS, focuses only on sagittal plane
Gait Assessment and Intervention Tool (G.A.I.T.)	Stroke patients	31 items: upper limbs, trunk, lower limbs in stance and swing phases	High sensitivity to therapy-induced changes, excellent reliability	Complexity limits routine use, better suited for research
Stroke Mobility Score (SMS)	Post-stroke patients	6 items: trunk posture, limb movements, gait speed, fluency, and stability	High inter-rater reliability, strong correlations with functional scales	Stroke-specific; limited utility for other conditions

The number of items evaluated in each index varies from six non-redundant items in SMS to 31 items in G.A.I.T. More comprehensive tools, such as G.A.I.T., evaluate gait in relation to a broad range of parameters by multiple body segments and over the gait cycle. This comprehensiveness can be an advantage in research and where detailed clinical evaluation is required [92] but may also make the tool more time consuming to perform and thus less practical in busy clinical settings or in a cursory screening situation. Indices that are more abbreviated, such as SMS, have increased efficiency and ease of use, which is particularly advantageous when routine clinical assessment is required or in situations in which clinicians have limited time [93].

VGA validity has been tested by correlating IGA and functional scale results. For example, EVGS had a good correlations with IGA measures and Gross Motor Function Classification System (GMFCS) functional scale results [84]. However, none of the identified VGA tools has the same consistency and precision as a fully instrumented gait analysis. Hip and pelvis movements can differ from quantitative measurements [8], likely due to visual perception of the combined movements of the hip and pelvis, which are particularly hard to perceive visually in the frontal and transverse plane.

Although many tools were originally designed for specific populations, such as children with CP or adults with stroke, many have since proven adaptable to other conditions and age groups [83], [84], [94], [95], [96]. For example, EVGS has been applied successfully across age and disorder groups other than the children with CP for whom it was originally designed and G.A.I.T., developed originally for stroke patients, has been used with multiple sclerosis patients [78]. However, validity for disorders other than those for which a tool was originally developed cannot be assumed and would necessitate additional studies to validate that claim [91].

The most consistent trend throughout the different VGA studies points out the influence of rater experience and the methodology of analysis on reliability. Indeed, many have reported significant improvement in inter-rater reliability following even very brief training sessions [97]. The methodology plays a critical role in reliability. The use of video recordings of gait, especially those that allow for slow-motion or freeze-frame analysis [22], [74], [98], improve consistency among ratings. Several studies reported that the use of specialized motion analysis software further improved agreement between raters on items dealing with joint angles and timing of such measurements [99].

According to a review paper, the PRS does not capture the whole pattern of gait accurately due to its wide range of variability and medium reliability [8]. WGS, RVGA, and G.A.I.T. are all sensitive to change following physiotherapy interventions and have good to excellent intra and inter-rater reliability [91]. While allowing a more differential assessment, using a five-point scale, the SF-GT may result in lower inter-rater reliability compared to other indices with simpler rating scales [77]. Although SMS has good reliability and good correlation with functional scales, it is limited by its specificity for stroke patients, hence limiting its applicability in other conditions [80]. Overall, The Edinburgh Visual Gait Score has emerged as a comprehensive analysis and reliable index. Because of the ability of this index to assess 17 parameters in multiple planes, it stands higher in capturing minute deviations, especially in pediatric CP individuals. And the score's ability to provide higher reliability for distal limb segments compared to proximal segments [52], [22], [84], [100].

2.5 Pose Estimation Models

Markerless pose estimation is a method for estimating the position and orientation of human and/or object without using a physical marker. Such an approach can be utilized in robotic, augmented reality, and biomedical fields [101], [102], [103]. Markerless approaches have several advantages over marker approaches, such as ease of installation, portability, and low cost, and for that reason, markerless approaches have a high potential for use in remote medical care [103]. Markerless body pose estimation offers convenient solutions compared to the traditional marker-based motion capture systems, utilizing a variety of techniques, from 2D binary silhouettes and skeleton models [104] to complex convolutional neural networks and multi-view video processing [105]. These techniques made human pose estimation possible from single images, video frames, or depth data for motion analysis and other applications, including health, robotics, and augmented reality.

Previous research was based on the fitting of 3D human body models to 2D image features, while more recently the combination of CNN-based segmentation with temporal priors (i.e., information or constraints from previous frames that help predict keypoints in the current frame over time) achieved high accuracy [106]. Depth images, together with efficient optimization techniques, have further improved real-time pose estimation [107]. Important advantages include robustness to occlusion [104], generalization across many diverse human poses [105], and realistic 3D shape avatars [106].

Pose estimation techniques can be divided into two broad categories: top-down and bottom-up. The top-down approach involves first detecting the person(s) in a frame and then estimating their poses. These are generally quite accurate but at a higher computational cost. In bottom-up approaches, individual body parts are detected first, followed by establishing correspondence between these parts with different persons. This involves sacrificing precision for speed [108].

The choice of pose estimation model depends upon the nature of the application required and the computational resources available. For instance, applications in which high precision is imperative, such as in clinical assessments, are best handled with top-down approaches, whereas applications requiring real-time processing, such as in crowd analysis, are more effectively done with bottom-up approaches [108]. Hybrid approaches could have advantages of both. For instance, [109] proposed a bottom-up hypothesis generation followed by a precise top-down analysis for estimating the hand pose, while [110] incorporated a bottom-up feature extraction followed by top-down parsing for improving the accuracy and speed. These hybrid frameworks thus illustrate the possibility of iterative refinement and activity-independent solutions in pose estimation.

Deep learning has completely changed the game for the pose estimation feature. Starting from CNNs, beginning with DeepPose to Adversarial PoseNet, models are building benchmark accuracies concerning robustness [111]. An extension of this concept further expands the area of applications toward behavior recognition, motion capture, human-computer interaction, and augmented reality [112]. Head pose estimation, as a sub-category of pose estimation, has grasped the limelight owing to its applications to facial analysis and emotion recognition tasks, [113].

2.5.1 OpenPose

OpenPose has emerged as a reliable tool for research and clinical applications, providing outstanding performance in multi-person pose estimation with anatomically accurate keypoints, and robust performance under a wide range of environmental settings. Clinical applications involving OpenPose have outperformed models such as HyperPose and BlazePose in ensuring high-quality pose inferences [114].

OpenPose is relatively slow as compared to the newer models, which include MoveNet, PoseNet, MoveNet Lightning, and Thunder [115]. However, despite all those disadvantages, its uniqueness

in multi-subject pose estimation within one frame is unparalleled. Furthermore, OpenPose had the lowest absolute error at 3.7 ± 1.3 (mean $\pm$ standard deviation), outperforming MoveNet Thunder (4.6 ± 1.8), MoveNet Lightning (5.9 ± 3.6), and DeepLabCut (6.8 ± 1.6) [116]. These absolute errors were computed by taking the difference between the pose estimation outputs and ground truth measurements obtained via marker-based motion capture systems. Hence, OpenPose is a good choice when high accuracy and multi-person tracking are required [117], [36], [118].

2.6 Automated Gait Analysis

Different approaches have been developed regarding the analysis and understanding of human gait patterns in automatic gait analysis. An automatic gait analysis method was developed using Rancho Observational Gait Analysis as the base for identifying movement deviations, but this system required a 3D motion analysis lab to provide gait data and lacked automatic reporting of EVGS results [119], which would limit access to the automated EVGS system to people who can attend a gait lab session.

Viswakumar et al. [120] proposed a markerless low-cost, easy-to-use approach using a mobile phone camera on a tripod and OpenPose to detect joint keypoints, but only calculated knee flexion/extension angles in their paper. For EVGS automation, more data is needed to calculate all 17 EVGS parameters.

The EVGS can be performed reliably with the aid of smartphone slow-motion video technology combined with a motion analysis application (Hudl), which enhances clinical usability by allowing the person to freeze a frame, draw lines, and measure angles [22]. While this could improve EVGS scoring, this approach does not provide automated scoring.

Ramesh et al. [23] proposed an automation method for performing EVGS using handheld smartphone video in combination with the OpenPose BODY25 body pose estimation model. The 2D joint keypoints were smoothed using a two-pass Butterworth filtering and linear interpolation to fill in missing values. The algorithm then determined the view (sagittal or coronal) and direction of motion (e.g., left-to-right, anterior-to-posterior) based on trunk length variation and nose keypoint trajectories. Gait events (foot strike, toe off, mid-midstance, mid-midswing) were detected using kinematic features derived from OpenPose keypoints. Foot strike was when the heel was maximally forward relative to the pelvis. Since OpenPose does not provide a sacrum keypoint,

the midhip keypoint was used as a proxy. Similarly, toe off was when the toe was furthest behind the midhip. Relative horizontal distances of heels and toes to midhip were used to make these detections. To detect mid-midstance and mid-midswing, Euclidean distance in frame space from right toe keypoints to left toe keypoints were calculated. Mid-midstance was indicated by minimal separation of toes in the frame, with maximal separation indicating mid-midswing. These events were used to define specific gait phases that were used to calculate EVGS parameters.

To calculate EVGS parameters, the algorithm derived joint angles and limb orientations based on geometric relationships between relevant body keypoints. For example, hip angle was the angle between a line perpendicular to the trunk axis (defined by midshoulder and midhip keypoints) and the thigh segment (hip to knee). Similarly, knee angles were the angle between the thigh and shank axes (hip-to-knee and knee-to-ankle lines). Ankle dorsiflexion/plantarflexion was the angle between the shank and foot axes (ankle-to-heel and heel-to-toe lines). Furthermore, other parameters, such as foot position at initial contact, trunk tilt, pelvic rotation, foot clearance, and lateral trunk shift were based on angular orientation and spatial relationships between body segments, using frames identified during gait events. For coronal plane parameters, such as pelvic obliquity and hindfoot valgus or varus, the algorithm inspected tilt and angular deviation of the pelvis and heel segments with respect to the image coordinate system.

The system was tested with able-bodied participants who were asked to reproduce different gait conditions for all EVGS parameters. The system had high Pearson correlations in 14 out of 17 parameters, where eight parameters had correlations greater than 0.8. Gait event detection accuracy ranged from two to five frames, while view detection accuracy exceeded 90%.

Despite promising results, the Ramesh study [23] had limitations since it was performed on a purpose-built dataset of able-bodied people who performed all EVGS parameter movements, which may not capture the full variability and complexity of pathological gait. The algorithm needs to be validated on a clinical dataset.

2.7 Conclusion

Many VGA tools have been developed to quantify and characterize abnormal gait, and several have become very useful in clinical settings, particularly for cerebral palsy assessments. Such

development represents an increasing demand for appropriate, reliable, and valid instruments that could easily be applied in a wide range of clinical situations. The Edinburgh Visual Gait Score provides reliability and validity, even for less experienced raters, thus enabling the examination of gait disturbances over a wide age range and spectrum of disorders. EVGS also correlates well with both IGA and functional scales, thus serving as an invaluable clinical tool.

Markerless pose estimation has opened new possibilities and opportunities for gait analysis. Advanced technologies such as convolutional neural networks and multi-view video processing have enabled human pose estimation from a single image, video frames, or depth data. Of these, OpenPose is the most reliable tool in research and clinical applications. OpenPose performance for multi-person pose estimation with anatomically correct keypoints predestines it for gait analysis in real-world conditions.

Recent advances have also seen these cutting-edge pose estimation techniques applied in conjunction with traditional gait indices, such as the EVGS. Automated versions of the EVGS, using OpenPose and smartphone video, have good agreement with human reviewers on most parameters. Technology integrated into a clinical assessment tool may make gait analysis more available and cheaper, with a possible expansion to use in even more varied clinical applications.

The study by Ramesh et al. [23] is currently the only published research that included a complete workflow for automatically calculating EVGS scores. However, this workflow needs to be evaluated with real-world clinical video before this approach can be confidently applied in practice.

3 Comparative Analysis of Gait Direction Detection Methods in Automated EVGS Implementation

EVGS automation requires accurate and reliable detection of walking planes and direction of gait. Ramesh et al.'s [23] previous study established initial methodologies for EVGS automation, where algorithms were tested on controlled datasets of able-bodied individuals who simulated gait for each EVGS score, with recordings made in controlled environments with stationary handheld smartphone cameras, good lighting, and stable frame rates. While working well for the able-bodied video dataset, Ramesh's method had poor performance when implemented on clinical videos of patients with pathological gait where the camera was moved to follow the person, camera zoomed as the person moved, or part of the person may move outside the video capture frame. These cases resulted in no EVGS score being provided or large errors in the provided EVGS parameter scores. This thesis was built on the original code from Ramesh and improved these methods to provide better function and robustness in a clinical dataset.

3.1 Plane Detection

In Ramesh et al.'s study [23], coronal or sagittal plane determination was based on the change in trunk length between the first and last frames of a video. A threshold value of 99 was used (i.e., if the difference in trunk length exceeded 99, the video was classified as coronal plane; otherwise, classification was sagittal). In the clinical recordings, camera zooming, patients moving toward or away from the camera, or unsteady video recording led to variations in trunk length. As such, relying on a single measurement between the initial and final frames leads to incorrect plane assignment.

This thesis provided a more resilient plane detection approach based on torso ratios generated from body keypoints. Unlike relative trunk lengths, which are affected by camera zoom and frame selection, torso ratios are computed on a per-frame level, thus making the system robust to changes in zoom level, as well as camera panning. This ensures that the algorithm classifies the correct plane, regardless of the level of proximity between the camera and the person or difference in the number of frames between videos. This shift toward a frame-wise calculation offers a more adaptable solution suitable for clinical video datasets.

3.2 Movement Direction Detection – Coronal

In the original methodology by Ramesh et al. [23], movement direction within the coronal plane was estimated using the difference in trunk length between the first and second last frames of a video. The assumption was that a person's trunk length would increase as they walk toward the camera and; conversely, trunk length would decrease as they walked away. In this manner, a negative trunk length difference indicated movement towards the camera and a positive value meant movement away from the camera. While this method worked well in static-camera setups, limitations have been found in clinical video scenarios with camera zoom, variable video conditions, and erratic camera movement. Zooming alters the trunk length, regardless of the direction of movement. In addition, since this approach compared only two frames from the entire video, if there is no patient in the first or second last frames, the approach will become invalid.

In this thesis, an enhanced frame-by-frame approach was developed to determine movement direction based on lateral (x-axis) joint coordinates. Specifically, the right hip, right knee, and right ankle average x-coordinates are compared with the average coordinates on the left side. If the average x-coordinate of the right leg is greater than the left leg, the person is walking away from the camera and, if less, the person is walking towards the camera.

The direction detection algorithm is applied to every frame in the video. The most frequent classification (mode) of the direction classifications for all frames is used to select the walking direction in the video. This approach allows the resulting movement direction classification to accurately reflect the most common movement direction, making it robust against outliers or zooming that might be present in real-world environments.

3.3 Movement Direction Detection – Sagittal

To determine movement direction in the sagittal plane, Ramesh et al. [23] calculated the difference between the nose x-coordinate in the first and the 75th frames of each video. If the difference was less than zero, the person was classified as moving from left to right and if greater than zero, the direction was classified as right to left. Even though this approach is computationally straightforward and successful for a fixed-camera setup, performance in real-world healthcare applications was greatly reduced.

Clinical walking videos often follow the patient through the walkway, especially in cases involving lengthy walkways. In such cases, the nose keypoint remains in the center of the frame, thus not providing a constant progression across the video field. Second, this approach assumed at least 75 frames in each video; however, if the video has a higher frame rate (60fps or more), and if the patient starts to walk after few seconds in the video, then at 0^{th} and 75^{th} frame, the patient might be standing at the same position making this algorithm detection invalid. Hence, exclusive use of two frames while ignoring the rest of the sequence drastically raises chances of incorrect labeling in real-world applications.

In this thesis a new method was developed based on lower body joint angles. To avoid issues for consistently detecting nose keypoints, the new approach uses the knee angle which is between knee-ankle and knee-hip for each frame. If the average knee angle over the entire video is greater than 180°, the person is walking left to right. If the average knee angle is less than or equal to 180°, the person is walking from right to left.

This approach has various benefits. It is independent of camera position and movement, not limited by fixed frame numbers (i.e., frames 0 and 75), and leverages all frames in the video to determine movement direction. It is, in turn, an improved technique for identifying sagittal plane direction in patient gait video.

3.4 Error Handling for Incomplete or Missing Foot Strike Data

Ramesh et. al.'s [23] algorithm detected gait events such as foot strikes, foot offs, and strides. Based on this foundation, new code in this thesis includes error-handling logic to improve algorithm robustness, since the original algorithm produced errors when analyzing videos from the clinical dataset. Specifically, the new code begins its process by checking if at least two complete strides were identified. If less than two strides were detected, the code checks for any foot strikes. If no foot strikes were detected, an error message is displayed, and further processing is terminated. If foot strikes were detected, the code checks for mismatches in left and right foot strikes. If no foot strikes were detected either on one side (i.e., either left foot strikes or right foot strikes) the code produces an error message about the absence of foot strikes for the specified side and processing is terminated.

3.5 Handling Poor Keypoints for Reliable EVGS Scoring

For Ramesh et. al. [23], low-confidence keypoints with a confidence score less than 0.5 were detected and removed. Subsequently, missing keypoints were interpolated to provide keypoints for each frame; however, if data gaps were abnormally extended then interpolation became impossible, leaving frames with missing keypoints.

Since EVGS parameters are calculated from specific sections of the video, such as at heel strike or midstance, updated code was implemented before calculating EVGS parameters to verify that all keypoints necessary for parameter calculations are available. If the essential keypoints for a parameter calculation are incomplete, the code exits and does not move forward with EVGS scoring. This step avoids inappropriately discarding videos with missing keypoints in areas where they do not affect parameter calculations.

4 Development and Validation of the Automated EVGS: Algorithm Development, Methodology and Evaluation Methods

4.1 Overview

This chapter presents the development of an algorithm for calculating EVGS and tests the algorithm on subset of videos from a clinical dataset. This chapter also presents the video processing steps and methodology adopted to automate the system. This chapter addresses Objective 1 of this research. The contents of this chapter will be submitted for publication. As first author, contributions include designing and implementing the automated EVGS calculation on CP participant videos, data processing, data analysis, and co-writing the manuscript.

4.2 Abstract

The Edinburgh Visual Gait Score (EVGS) is a commonly used clinical scale for assessing gait abnormalities, providing insight into diagnosis and treatment planning. However, its manual implementation is resource-intensive, requires time, expertise, and a controlled environment for video recording and analysis. To address these issues, an automated approach for scoring the EVGS was developed. Unlike past methods dependent on controlled environments or simulated videos, the proposed approach integrates pose estimation with new algorithms to handle operational challenges: camera movement, variable zoom, and partial visibility of the patient. The system uses OpenPose for pose estimation and new algorithms for automatic gait event detection, stride segmentation, and computation of the 17 EVGS parameters across the sagittal and coronal planes. Evaluation with gait videos of cerebral palsy patients showed high accuracy for parameters such as hip and knee flexion but indicated a need for improvement in pelvic rotation and hindfoot alignment scoring. This automated EVGS approach can minimize workload for clinicians through the introduction of immediate gait analysis and enable mobile-based applications for clinical decision-making.

4.3 Introduction

Gait analysis is an essential tool for understanding human locomotion and diagnosing movement

pathologies. In particular, gait analysis is a pillar in the orthopedic management and treatment of ambulatory children with cerebral palsy (CP) [121]. Recent developments have highlighted the utility of clinical gait evaluation with visual assessment [122].

Visual Gait Analysis (VGA) is effective for assessing gait in children with CP, providing information on functional mobility when other advanced tools are not available [54]. The Edinburgh Visual Gait Score (EVGS) is a valid, objective, gait assessment tool, specifically for people with CP [8]. EVGS has modest correlations with functional mobility tests, including the Timed Up and Go Test and Gross Motor Function Classification System [123]. Furthermore, EVGS links impaired selective voluntary motor control in CP children to key gait parameters, including foot clearance and maximum ankle dorsiflexion during the swing phase [124]. Moderate correlations between EVGS and trunk motions highlight the utility of EVGS to capture functional features of gait modulations [124]. EVGS can increase the usability and affordability of gait analysis, such that analyses can be practically implemented in a variety of clinical environments [125]. Robinson et al. [82] determined the minimal clinically important difference (MCID) of EVGS to be 2.4, which corresponds with assessment tools based on functional observation (e.g., Gross Motor Function Classification System). These results confirm the utility of VGA, and particularly EVGS, for the diagnosis and quantification of gait irregularities in CP patients.

EVGS use can be resource-intensive since time and expertise are required for implementation. Furthermore, a controlled environment is required for video recording and analysis. However, research using digital tools to calculate EVGS is paving the way for accessible and efficient gait analysis in clinical practice. Aroojis et al. [22] showed the viability of applying smartphone slow-motion video and motion analysis software (Hudl app) to effectively implement the EVGS. The joint angles were calculated from the software and EVGS was scored manually. The average time to calculate the EVGS was 24.7 min (16–55 min). Ramesh et al. [23] utilized OpenPose-based algorithms for EVGS score extraction from smartphone videos and demonstrated good correspondence with human reviewers for the majority of parameters. However, Ramesh's approach was not validated with patient videos, where video acquisition may occur under less controlled conditions. Nevertheless, these advances demonstrate the promise of automated EVGS systems for standardized gait assessment, enhanced efficiency, and expanded use of gait assessment with cerebral palsy patients in everyday clinical practice.

This study presents and evaluates an efficient system for automatic event detection, stride segmentation, and EVGS scoring from 2D videos of patient gait. These real-world videos present technical issues that are analogous to the problems that clinicians must address when managing patient video data in practice. An efficient and accurate system could alleviate the clinician workload by reducing or eliminating the need for manual intervention when scoring EVGS trials. Such an automated approach would also enhance patient accessibility to gait analysis since video could be captured at the point of patient contact.

4.4 Algorithm Development

To achieve automated EVGS analysis, the proposed system must identify the appropriate video frames for analysis and then apply a series of rules to generate scores for each parameter. Specific gait events in walking videos must be detected, and an algorithm capable of scoring EVGS parameters must be implemented. The proposed approach involves a sequential pipeline that includes pose estimation, plane detection, movement direction determination, gait event identification, stride segmentation, and the algorithmic computation of EVGS scores.

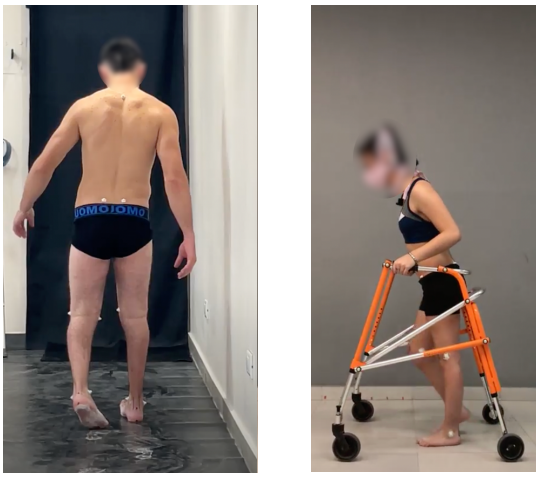

(a) (b)

Figure 4.1 Sample videos in (a) coronal and (b) sagittal planes

A video dataset of patient gait from Sanatorio del Norte medical center in Tucumán, Argentina was used for EVGS algorithm development and evaluation. The set provided sagittal and coronal view gait videos for 230 people with walking disorders. Videos were recorded at 60 Hz and were captured in a closed environment with good lighting (Figure 4.1). Markers were located on joints

to assist the manual evaluators with EVGS scoring. Our research group's previous experience with OpenPose showed no effect of markers on the person for keypoint identification. This private dataset is not publicly available.

4.4.1 Qualitative Video Assessment

To work with appropriate videos for algorithm development, the Sanatorio del Norte's patient sets were qualitatively assessed to select videos that were suitable for automated EVGS development, including sagittal and coronal views. Videos were screened based on absence of multiple individuals within the frames, lack of an overhead camera operator in the frame (i.e., overhead camera operator was occasionally in the field of view), clear coronal or sagittal view, minimal zooming during recording, and full body visibility. When possible, videos were cropped or trimmed to isolate the patient in the video (i.e. remove sections where people were helping the patient or an overhead cameraman was visible in the frame). A total of 50 patient sets met the inclusion criteria. Of these, the first 20 sets were used exclusively for developing the algorithm and were not included in testing, while the remaining 30 sets were used to validate the algorithm.

4.4.2 Video Processing

Figure 4.2 shows the general methodology for the automated algorithm. The process begins with a qualitative assessment of the patient sets, using the criteria in section 4.4.1. Patient sets that do not meet these standards were further reviewed to determine if they could be adjusted for usability. Patient sets that could not be adequately cropped or trimmed were rejected from further analysis. The next step involves pose estimation using OpenPose, a well-established pose estimation model [17], [126], [127]. The OpenPose BODY25 model detects 2D body keypoints on the head, trunk, and limbs (Figure 4.3). Python was used to perform the computations.

Once pose estimation is completed, the system performs direction detection to determine if the person is walking left-to-right or right-to-left in sagittal plane or moving towards or away from the camera in the coronal plane. Subsequently, the algorithm identifies whether the video is recorded from a sagittal (side) or coronal (front/back) perspective. Following direction and perspective identification, the system detects gait events, such as heel strikes and toe-offs, using the method reported by Ramesh et. al. [23]. Stride detection builds on gait event detection by identifying

complete strides, from one heel strike to the next heel strike on the same foot. All subsequent processing is performed on each stride. Following stride detection, EVGS scores for each stride are calculated for 17 parameters (12 sagittal and 5 coronal). Then, the EVGS algorithm is applied to the pose estimation and gait event data to generate scores for each video.

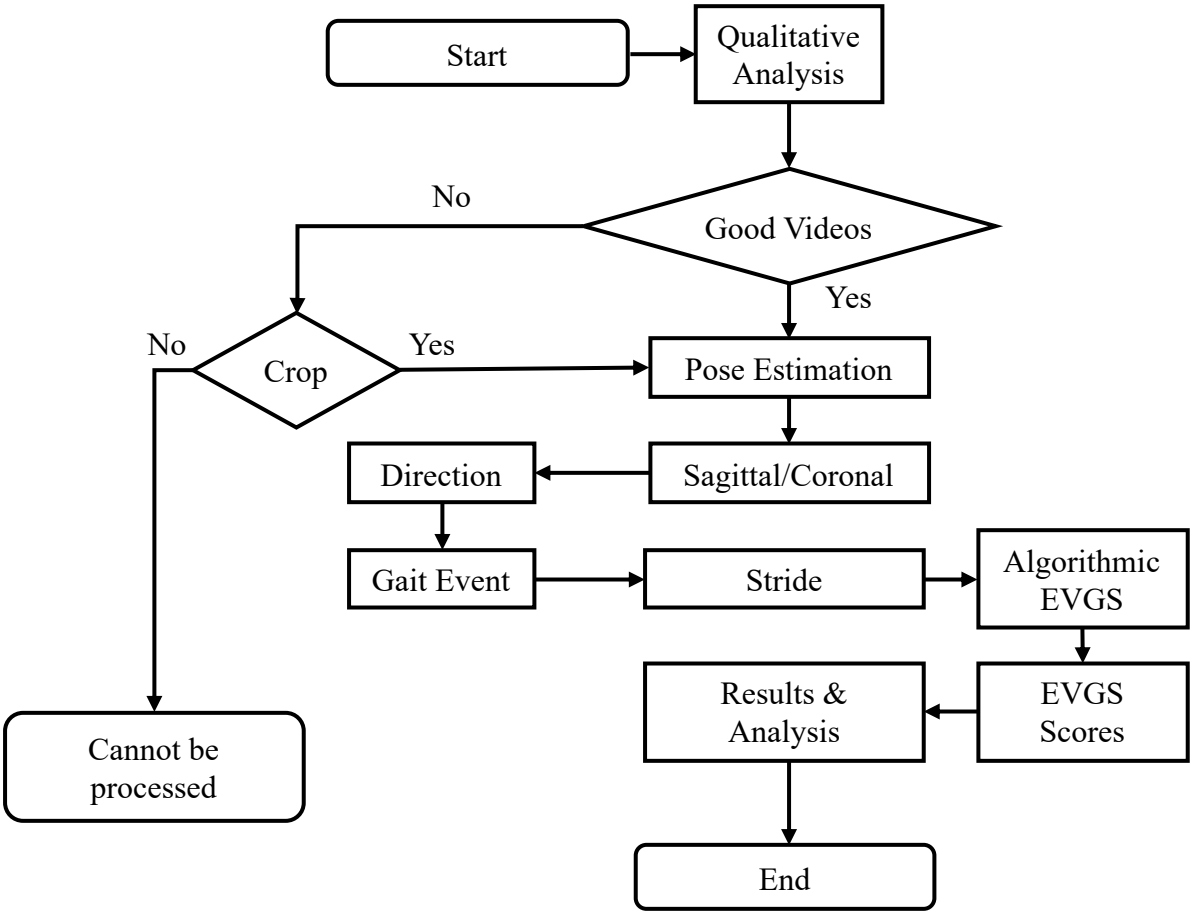

Figure 4.2 Flowchart of the overall algorithm

Keypoint Processing

Since the raw keypoint coordinate trajectories often contain noise and sometimes outliers, keypoint time series were filtered using a zero-phase, dual-pass, second-order Butterworth filter with a 12 Hz cut-off frequency. 2D keypoint processing was adapted from a previously established markerless Artificial Intelligence (AI) motion analysis methodology for hallways [128]. Keypoints with confidence scores below a 10% threshold were excluded, and any resulting gaps up to five frames (0.083 seconds) were interpolated using cubic spline interpolation [129]. Any frames that still had poor keypoint accuracy were not processed.

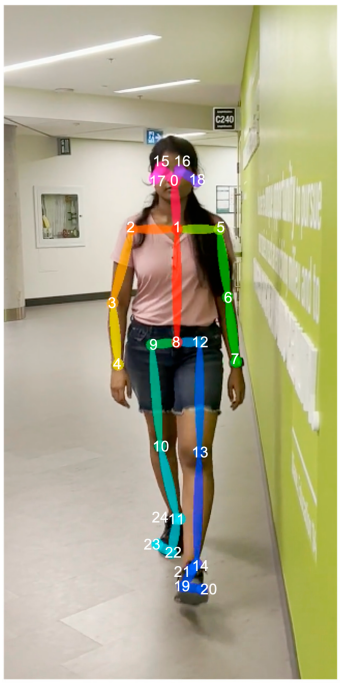

Keypoints	Body parts
KP0	Nose
KP1	Mid shoulder
KP2	Right shoulder
KP3	Right elbow
KP4	Right hand
KP5	Left shoulder
KP6	Left elbow
KP7	Left hand
KP8	Mid hip
KP9	Right hip
KP10	Right knee
KP11	Right ankle
KP12	Left hip
KP13	Left knee
KP14	Left ankle
KP15	Right eye
KP16	Left eye
KP17	Right ear
KP18	Left ear
KP19	Left big toe
KP20	Left small toe
KP21	Left heel
KP22	Right big toe
KP23	Right small toe
KP24	Right heel

Figure 4.3 OpenPose human pose estimation using BODY25 model

Coronal/Sagittal Plane Detection

As shown in Figure 4.4, torso ratios are used to distinguish the sagittal view from the coronal view videos. These ratios are based on the spatial ratios between the shoulders and hips, since variations in these ratios can provide information about the body's orientation with respect to the camera.

For each frame, R_1 is the ratio of the distance between the left shoulder and left hip to the distance between the right and left shoulders (Eq 4.1).

$$R_1 = \frac{\sqrt{\left(x_{left\_shoulder} - x_{left\_hip}\right)^2 + \left(y_{left\_shoulder} - y_{left\_hip}\right)^2}}{\sqrt{\left(x_{right\_shoulder} - x_{left\_shoulder}\right)^2 + \left(y_{right\_shoulder} - y_{left\_shoulder}\right)^2}} \quad (4.1)$$

For each frame, R_2 is the ratio of the distance between the right and left shoulders to the distance between the right shoulder and right hip, assessing the upper body width relative to the vertical length of the right side (Eq 4.2).

$$R_2 = \frac{\sqrt{\left(x_{right\_shoulder} - x_{left\_shoulder}\right)^2 + \left(y_{right\_shoulder} - y_{left\_shoulder}\right)^2}}{\sqrt{\left(x_{right\_shoulder} - x_{right\_hip}\right)^2 + \left(y_{right\_shoulder} - y_{right\_hip}\right)^2}} \quad (4.2)$$

Finally, R_3 is calculated as the ratio of the previous two ratios

$$R_3 = \frac{R_1}{R_2} \quad (4.3)$$

The (per video) mean of the (per-frame) R_3 values is calculated and used for the "coronal or sagittal" decision.

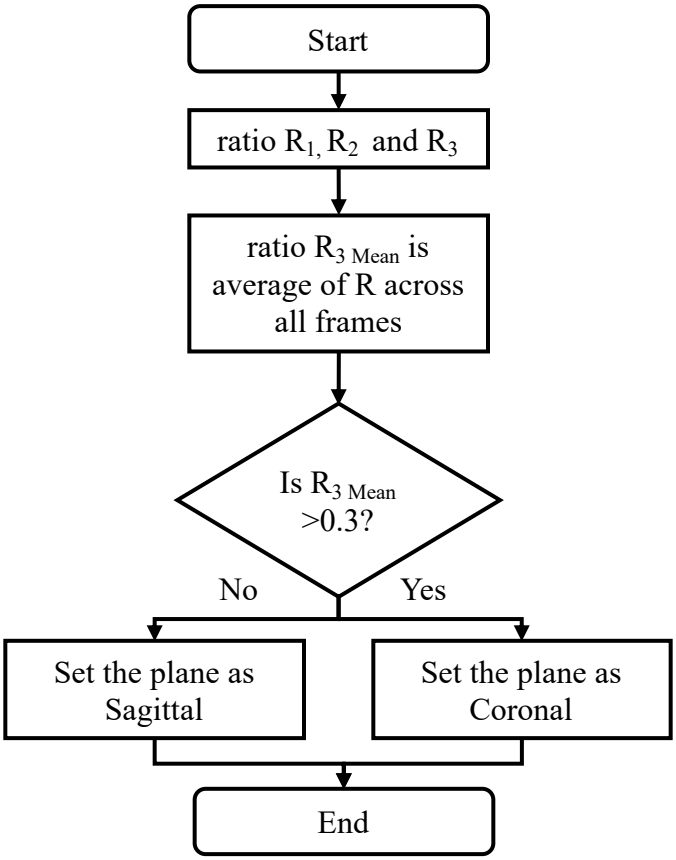

Figure 4.4 Flowchart depicting the detection of sagittal/coronal plane view

The average R_3 value for a video ($R_{3\ Mean}$) was calculated by averaging the R_3 values from all

frames in the video. A decision rule is used for coronal/sagittal plane classification, such that if $R_{3\ Mean}$ is greater than 0.3 the view is classified as sagittal. If $R_{3\ Mean}$ is less than or equal to 0.3, the view is coronal. This threshold was determined based on analysis of 20 videos used during algorithm development, where the threshold was iteratively adjusted to maximize classification accuracy across a range of body types and video angles.

Movement Direction

In the sagittal plane, the process for detecting movement direction (Figure 4.5) starts by calculating the knee angle for each video frame, using the hip, knee, and ankle joint coordinates (Eq 4.4). The numpy $arctan2(y,x)$ function computes the angle between the positive x-axis and a vector from the origin to the point (x,y) in two-dimensional Cartesian space. Unlike the standard arctangent function $arctan(y/x)$, $arctan2$ considers the signs of both (x) and (y) to determine the correct quadrant of the angle, making it more robust for applications involving directional calculations. In (Eq 3.4), the first $arctan2$ term calculates the angle of the line segment between the knee and the ankle, while the second $arctan2$ term calculates the angle of the line segment between the knee and the hip. Subtracting these angles gives the relative joint angle at the knee.

Let A_{rh_rk} and A_{ra_rk} represent the vectors between the hip, knee, and ankle. The directional angle θ_i for each frame i is calculated as

$$\theta_i = arctan2(y_{ankle} - y_{knee}, x_{ankle} - x_{knee}) - arctan2(y_{hip} - y_{knee}, x_{hip} - x_{knee}) \quad (4.4)$$

Knee angles are calculated for the right leg, and the average angle for the right leg is calculated for the entire video.

A decision rule based on threshold values is used to classify the movement direction. A threshold of 180° was selected from empirical observation of the development video set. If Mean Knee Angle > 180°, then the direction of movement is right to left. If the Mean Knee Angle ≤ 180°, the motion is classified as left to right.

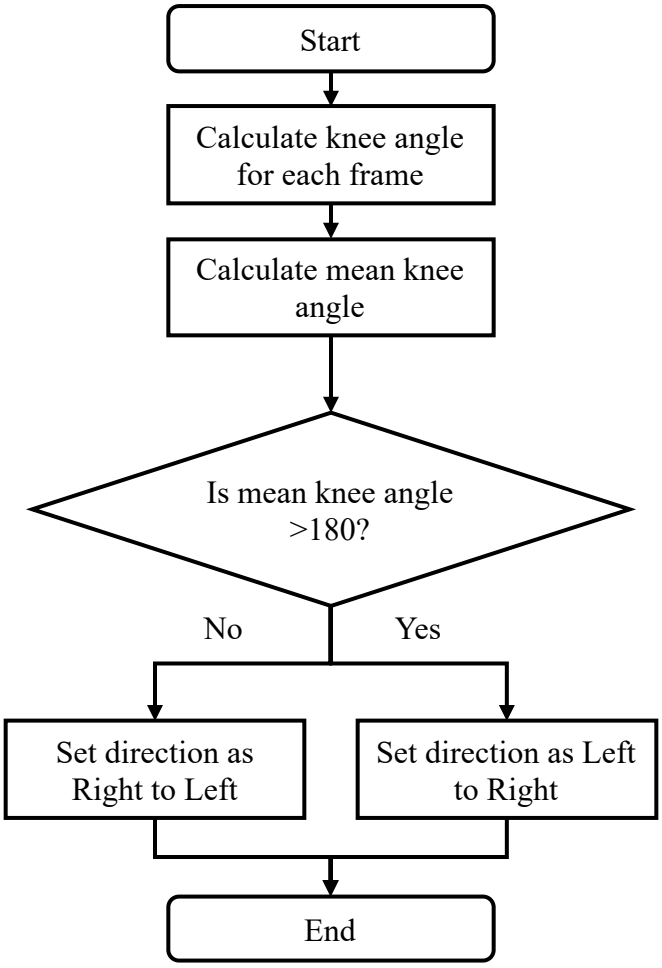

Figure 4.5 Flowchart to identify direction of movement in the sagittal plane

The coronal detection process is shown in Figure 4.6. For each frame in the video, x-coordinates of hip, knee, and ankle are extracted for both legs. Right leg average is the average x-coordinate for the 3 right joints. Left leg average is the average x-coordinate for the 3 left joints. If the right leg average is greater than the left leg average, the person is walking away from the camera. If the right leg average is less than the left leg average, the person is walking towards the camera. After calculating the direction for each frame, the most frequent classification (mode) of the direction classifications for all frames is used to select the walking direction in the coronal plane

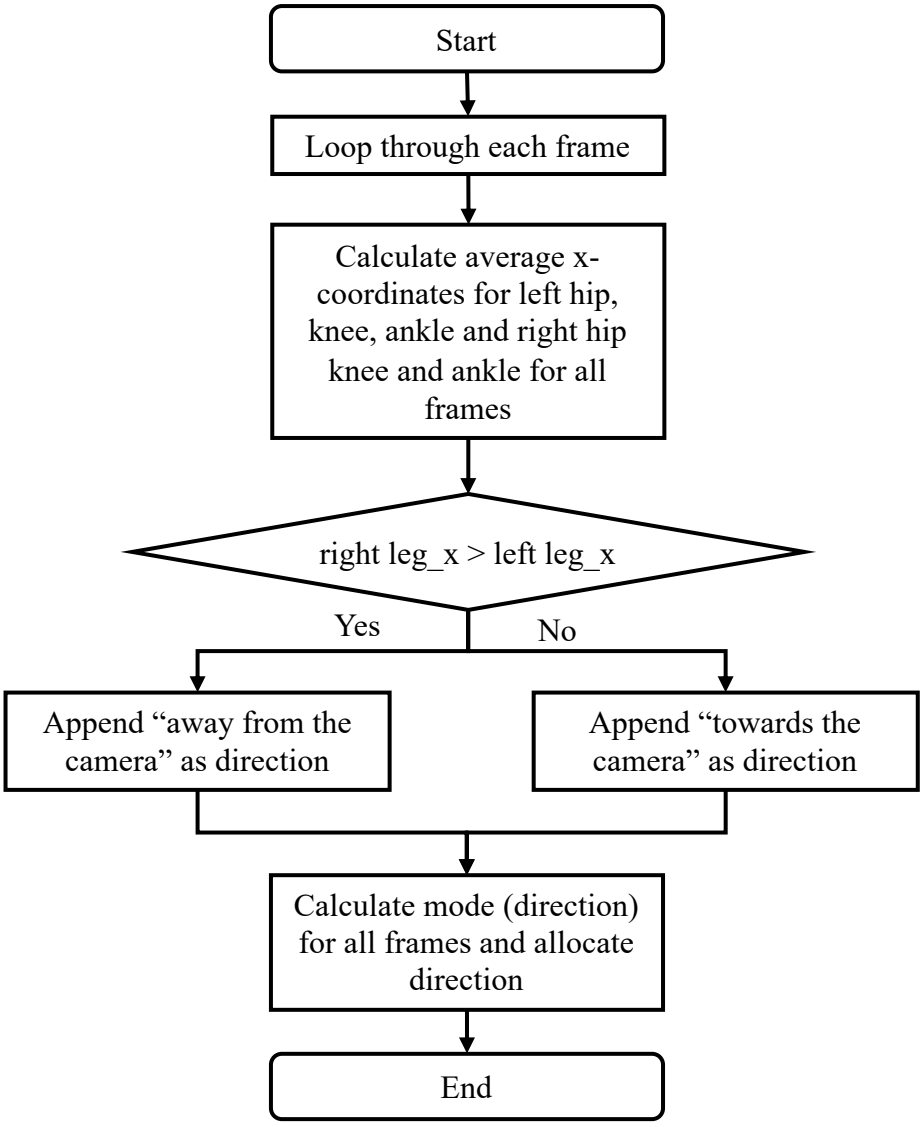

Figure 4.6 Flowchart to identify direction of movement in the coronal plane

4.4.3 EVGS Parameters

The Edinburgh Visual Gait Score has 17 parameters for each of the two lower extremities, totaling 34 parameters. Commonly, sagittal and coronal views of a patient are recorded with a handheld camera, or one attached to a tripod. These videos are then manually scored by clinicians in accordance with the EVGS guidelines. During scoring, video editing software is often used to pause the video at relevant gait events for detailed analysis. Software tools can also be used to calculate joint angles and other parameters relevant to EVGS. Each EVGS parameter is scored on a 3-point ordinal scale: 0 indicates normal gait (within ±1.5 standard deviations of the mean); 1, moderate

deviations (1.5 to 4.5 standard deviations from the mean), and 2, significant or severe deviations (more than 4.5 standard deviations from the mean) [50]. A low total score reflects fewer gait deviations. To facilitate a clear understanding and to ensure consistency in scoring, the 17 EVGS parameters were grouped according to foot events and gait cycle phases (Table 4.1).

Table 4.1 EVGS parameters [23]

	Foot events and gait phases	**EVGS parameters**
Sagittal	Initial contact/Terminal swing	Peak hip flexion in swing
		Knee extension in terminal swing
		Initial contact
	Midstance	Peak sagittal trunk position
		Pelvic rotation in midstance
		Heel lift
	Terminal stance	Peak hip extension in stance
		Peak knee extension in stance
		Max ankle dorsiflexion in stance
	Midswing	Peak knee flexion in swing
		Maximum ankle dorsiflexion in swing
		Foot clearance in swing
Coronal	Midstance	Maximum lateral shift of trunk
		Maximum pelvic obliquity in stance
		Knee progression angle
		Foot rotation
		Hindfoot valgus/varus

Most EVGS parameters require joint angles. The ankle, knee, hip angles were calculated using the method reported by Ramesh et al.[23].

4.5 Evaluation

4.5.1 Methods

30 patient sets from the algorithm development dataset were reserved for algorithm evaluation.

Algorithm performance for sagittal and coronal planes were assessed by comparing the algorithm results with manual classification of movement plane and movement direction. Accuracy, sensitivity, specificity, precision and F1 score were calculated to validate the algorithm's

effectiveness for plane and movement direction detection. One examiner reviewed all videos to extract the ground truth planes and directions.

EVGS scoring was evaluated by comparing algorithm outcomes to manual EVGS scores that accompanied videos in the Sanatorio del Norte dataset (i.e., experts at Sanatorio del Norte hospital used sagittal, coronal, and overhead views to score EVGS for each video). Accuracy was calculated for each of the 17 EVGS movements using (Eq 4.5)

$$Accuracy = \frac{Number\ of\ patients\ correctly\ classified}{Total\ number\ of\ patients} \tag{4.5}$$

A correct classification occurred when the EVGS algorithm score matched the ground truth score. Accuracy was calculated for right and left legs separately and then the accuracies were averaged between legs for each of the 17 parameters. Accuracy was the metric used to compare EVGS scores. For this study, high accuracy was 85%-100%, moderate accuracy was 70%-85%, and less than 70% was considered low accuracy.

4.6 Results

4.6.1 Coronal/Sagittal View Detection

Coronal and sagittal detections were correct for all patient sets (100% accuracy, 100% sensitivity, 100% specificity, 100% precision, F1-score of 1).

4.6.2 Direction of Motion Detection

Direction of motion detection in the sagittal plane was correct for all right-to-left movements and 28 of 30 left-to-right movements (96.67% accuracy, 100% sensitivity, 93.75% specificity, 93.33% precision, and F1-score of 0.96). The 2 misclassifications were because of multiple candidates in the video or excessive zooming.

Direction of motion detection in the coronal plane was correct for all videos (100% accuracy, 100% sensitivity, 100% specificity, 100% precision, and F1-score of 1).

4.6.3 EVGS Scoring

Figure 4.7 (sagittal) and Figure 4.8 (coronal) show EVGS outcomes for accuracies averaged between right and left legs. Peak hip flexion in swing, peak knee flexion in swing, maximum ankle dorsiflexion in swing, and maximum pelvic obliquity in stance had the best accuracies (90-97%). Initial contact, maximum ankle dorsiflexion in stance, peak sagittal trunk position, knee progression angle, and foot rotation also had high accuracies (82-89%).

Moderate accuracy (71-75%) was seen for knee extension in terminal swing, heel lift, peak knee extension in stance, peak hip extension in stance, foot clearance in swing, and maximum lateral shift of the trunk. Pelvic rotation in midstance and hindfoot valgus/varus had the lowest accuracy (52-53%).

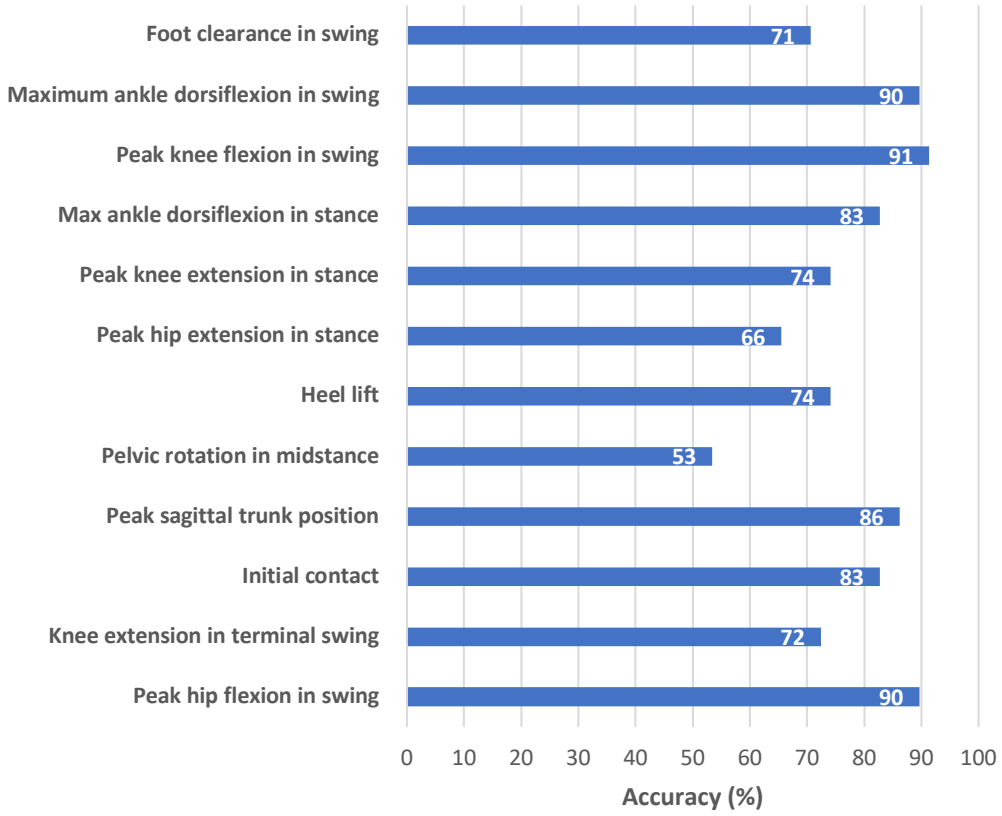

Figure 4.7 Accuracy between algorithm and ground truth for sagittal view parameters

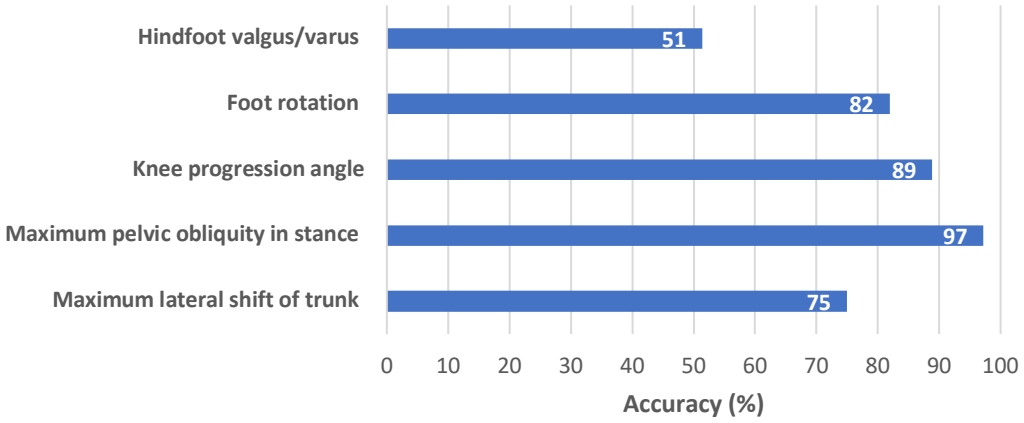

Figure 4.8 Accuracy between algorithm and ground truth for coronal view parameters

4.7 Discussion

A viable algorithm was produced that automatically calculated the EVGS score from sagittal and coronal videos of people with gait disorders. High accuracy was achieved for most EVGS parameters, but further development could improve results for out-of-plane movements.

4.7.1 Sagittal Plane Parameters

The majority of EVGS parameters had high accuracy and therefore were equivalent to manual EVGS scoring. Heel lift and foot clearance had moderate accuracy. Events like foot strike and foot-off are necessary to determine the heel lift score. Hence, this score is sensitive to small changes in these gait events. Ramesh et al. [23] reported that changes of only one frame could result in the score changing from a 0 to 1. In future research, another method of scoring heel lift could be considered, where the score is less dependent on stride events and more related to inter-limb kinematics.

The foot clearance parameter had moderate accuracy. Human reviewers usually determine the foot clearance score by finding the video frame where the foot looks to be closest to the ground, and then determining the score [81]. The algorithm is slightly different, since the method does not try to calculate a ground plane, which would be used to determine the distance from the foot markers to the ground. For the algorithm, full clearance is defined as when the big toe and heel of the swing

leg crosses the big toe and heel of the contralateral stance leg (e.g., when walking left to right, the x-coordinates for both the left heel and big-toe are greater than the x-coordinates of both the right heel and big-toe) [23]. This ensures that any video (e.g., hand-held, etc.) can be processed by the automated system. These differences in approach may result in some discrepancies for cases with small foot clearances.

Knee extension in terminal swing and peak knee flexion in stance had moderate accuracy. Out of the 30 patients, 10 had high accuracy, 10 had low accuracy, and 10 had medium accuracy. Since clinicians can find it difficult to detect small angular differences, such as between 14° and 17° (e.g., knee extension in swing angle of 5° to 15° corresponds to a score of one; angles between 16° and 30° score as two), inter-rater differences for parameters that are close to the transition between scores can occur. Since the algorithm calculates quantitative joint angles, the algorithmic approach may provide more consistent results for these cases. Further research with a larger dataset will help to confirm algorithmic scoring consistency.

Pelvic rotation in midstance and peak hip extension in stance had the lowest accuracies. OpenPose provides hip keypoints; however, it does not provide sufficient landmarks to determine pelvic segment orientation. Instead, the angle of pelvic rotation was calculated with a line joining the right and left hip joints relative to the y-axis (vertical) of the sagittal plane from the image coordinate system [23]. Other surrogate measures could be investigated, such as inter-hip distance changes in the coronal plane. As well, new pose detection methods that estimate depth axis could be investigated to improve automated EVGS scoring for these transverse plane movements.

Similarly, for peak hip extension, the hip angle is defined as the angle between the trunk axis and the thigh axis, since OpenPose does not provide keypoints to define a pelvis segment. The trunk axis is a line connecting the neck and mid-hip keypoints, while the thigh axis uses the hip and knee keypoints. Human scorers interpret hip extension as the thigh angle relative to the pelvis. Trunk angle can differ from pelvis angle during gait, especially for pathological gait where the trunk can be bent over and have a much greater range of motion. Therefore, clinician assessment can differ from the algorithm scoring.

4.7.2 Coronal Plane Parameters

Coronal view parameters had generally good accuracy of all five parameters. Maximum pelvic obliquity in stance and knee progression angle had high accuracy.

Foot rotation and lateral trunk shift had moderate agreement between algorithm and ground truth. Studies have consistently shown that EVGS reliability is higher for distal segments (foot, ankle, knee) compared to proximal segments (trunk, pelvis, hip) when assessing gait abnormalities in children with cerebral palsy [22], [83], [84]. Therefore, some of the differences for trunk shift could be attributed to manual scoring.

Hindfoot valgus/varus had low accuracy due to challenges in keypoint detection. In the coronal view, heel and toe keypoints tend to cluster or overlap or are occluded by the big toe keypoint (Figure 4.9). Ankle and heel keypoints are close to each other, and the inter-keypoint distance becomes smaller as the person walks away from the camera. Hence, these keypoints are more likely to be occluded during gait, which will result in scoring discrepancies. It is worth noting this is not a problem with the algorithm alone since humans also find it challenging to estimate foot keypoints under such conditions [23]. These factors can also affect foot rotation scoring.

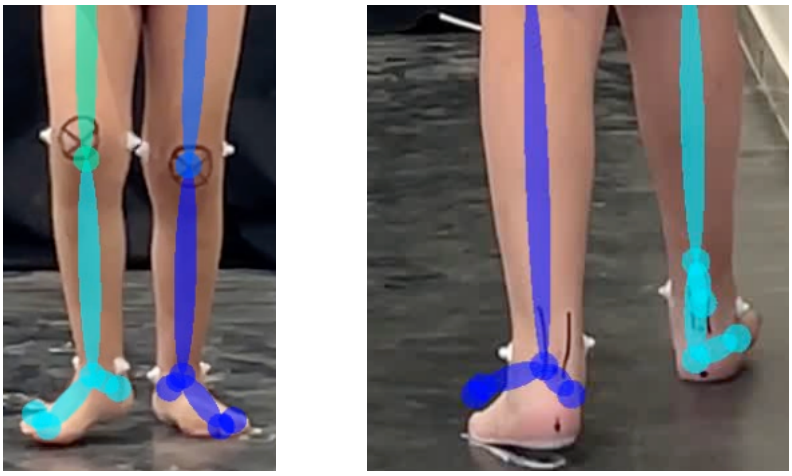

(a) (b)

Figure 4.9 Overlapping of foot keypoints (a) walking towards the camera and (b) walking away from the camera

The study has several limitations that should be acknowledged. First, participants were between 6 to 40 years of age. Encompassing both pediatric and adult populations introduces diversity that,

while valuable for broader evaluation, may have affected the algorithm's consistency. Although the EVGS was developed for children with CP, tuning the algorithm specifically for pediatric or adult participants could produce better results. Physical differences between children and adults, such as variations in body size, proportions, and movement dynamics, may not fully fit the ranges set by the EVGS for a given pediatric population. This can reduce the algorithm accuracy and its generalizability across different age groups. In future work, adapting algorithmic approaches for pediatric or adult populations will require larger datasets. Moreover, the algorithm was not tested against diverse patient ethnicities or scenarios involving multiple participants, which could result in errors in identifying the primary subject or tracking their movements. The algorithm was not tested against various backgrounds or the presence of more than one person in the video, either of which could result in errors in identifying the primary person or tracking their movements.

4.8 Conclusion

This chapter presents an automated methodology for applying EVGS to patient data, testing the effectiveness of the EVGS scoring algorithm compared to expert scoring. Automatic stride detection and movement direction detection performed well in both the sagittal and coronal videos, while EVGS performance varied between parameters. Of the 17 EVGS parameters, high accuracy was calculated for nine, moderate for six, and low for two parameters. Refinements are still required for accurate classification of pelvic rotation at midstance and hindfoot valgus/varus. This automated approach is suitable to process the patient video data, and thus is promising for automating clinical gait analysis, thereby increasing the availability of gait evaluation and enabling patient monitoring outside clinical environments.

5 Automated EVGS Testing

5.1 Overview

This chapter reports on algorithm testing with a larger unseen CP patient clinical dataset (i.e., different people than the development dataset) and demonstrates the algorithm's potential to provide accurate EVGS results for clinical decision-making. This includes accuracy between algorithm and ground truth outcomes and the effect of being the same or being within one score of ground truth. This chapter addresses Objective 2 of this research. The content of this chapter will be submitted for publication. As the first author, contributions include testing the automated scoring system, performing analysis, and co-authoring the manuscript.

5.2 Abstract

The Edinburgh Visual Gait Score (EVGS) is a validated clinical tool for assessing gait abnormalities, particularly for people with cerebral palsy (CP). However, manual scoring is time-intensive and subjective, necessitating automated solutions. This study validated an automated EVGS scoring system with patient videos acquired in a CP clinic. Leveraging pose estimation, gait event detection, and stride analysis, the system processes coronal and sagittal plane videos to compute EVGS parameters. Tested on 89 clinical video sets of patients with cerebral palsy, the algorithm demonstrated high accuracy in stride detection, movement direction classification, and EVGS scoring. Use of clinical videos introduced challenges to automated scoring. Eleven of the 17 EVGS parameters achieved accuracy rates between 84–94%, while four had moderate accuracy, and two parameters had low accuracy. EVGS automation reduces the time and effort required for gait assessment, offering a viable alternative to manual scoring for efficient gait outcome measurement.

5.3 Introduction

Advancements in automated gait analysis have a high potential for enhancing clinical decision-making, particularly for cerebral palsy (CP) patients, who present with gait abnormalities. The prior chapter introduced an algorithm for automating EVGS scoring for gait videos taken in a clinic, with a view to enhancing the accuracy of EVGS parameters and providing an effective tool for use in clinical decision-making for CP patients. In this chapter, a large and heterogeneous CP patient

dataset was utilized to evaluate algorithm performance under real-world clinical conditions.

Implementing an automated system in a clinical setting involves unknowns and challenges. Clinical settings may introduce variation in terms of video quality, participant compliance, and environment (i.e., lighting, occlusions that occur in an unpredictable manner, camera factors, etc.). In addition, heterogeneity in CP gait patterns, including differences in severity, use of walkers, and compensatory motions, adds complications not encountered with an able-bodied participant dataset. Perhaps most importantly, the algorithm ideally generalizes to a variety of clinical settings, with variation in equipment, protocols, and expertise of the examiners that can contribute to variation in video capture and scoring standards.

This study assessed whether the automated algorithm can effectively work with large and heterogeneous video datasets (e.g., walkers, different levels of gait abnormalities) representative of routine clinical settings. The algorithm was also evaluated as a potential clinical decision-making tool by comparing performance with expert-rated benchmarked scores. Critical information regarding efficacy, usability, and potential integration into routine clinic workflows was derived from this study.

5.3.1 Technical Challenges of Using Patient Videos

To test the EVGS scoring algorithm in clinical conditions, a dataset of clinical videos was obtained from Sanatorio del Norte hospital, Tucumán, Argentina. This dataset provided sagittal, coronal, and transverse view gait video for 230 people with walking disorders. Only sagittal and coronal videos were used by the automated EVGS system, to ensure that the system can be used in typical clinical environments where transverse plane video is not available. Upon reviewing the Sanatorio del Norte medical center dataset, various challenges for automated analysis were observed, such as the camera moving with the patient, variable zooms, partial views of the patient (often missing head and trunk), or the presence of multiple people assisting the patient (Figure 5.1). Each of these factors presents a unique obstacle in implementing a fully automated EVGS assessment for gait analysis in clinical practice.

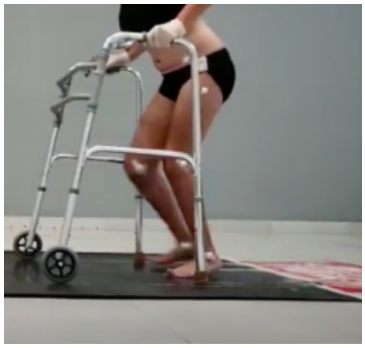

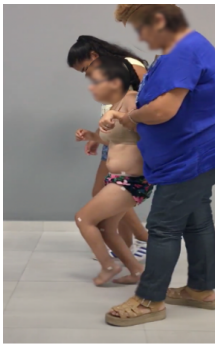

(a) (b) (c)

Figure 5.1 Challenges in patient data (a) head/trunk missing and (b) multiple people assisting patient, coronal view (c) multiple people assisting patient, sagittal view

In clinical settings, videos are usually recorded by a technician or clinician who moves the camera to keep the patient within the frame. However, this introduces video instability and angle variability, complicating the task for algorithms that assume a fixed-camera viewpoint. Consequently, this may affect automatic body keypoint tracking, especially in stride length, foot placement, and gait parameter calculation. However, algorithmic approaches may consider these shifts and provide appropriate results, as discussed in section 3.3

Zooming can also be a problem since frequent zoom adjustments make it difficult for algorithms to track keypoints between frames with high accuracy and consistency. Another common problem in clinical videos is partial visibility of body segments, such as missing head and/or trunk regions across various parts of the videos. This problem results from clinicians often framing the camera to capture only legs and feet. However, for automation, the absence of the head or trunk can interfere with proper calculation of gait-related parameters that depend on a complete view of the body, and also adversely affect pose detection model keypoint identification.

Frames with multiple people assisting a patient are common in videos involving patients with severe mobility limitations, such as cerebral palsy. This may include one or more people in the frame who are physically supporting or stabilizing the patient, thereby obscuring the patient and adversely affecting keypoint identification. Processing only the strides that are not influenced by extraneous figures can improve EVGS computation accuracy.

Each of these technical challenges, although individually complex, are surmountable on their own with appropriate software. The methods in this research enabled automated EVGS scoring even with the head missing from the video frame, small zoom changes, and the camera moving with the

patient.

5.4 Methods

A qualitative review of the video dataset was performed to evaluate and refine the dataset, selecting only videos that met established quality criteria while excluding any that may otherwise introduce artifacts into the system (i.e., videos that would be excluded in practice). The videos were screened for multiple individuals in the frame, camera operator in the frame, and failure to record the full body (i.e., head to toe).

Videos were trimmed into sagittal (person walks left to right, person walks to right to left) and coronal (person walks towards the camera, person walks away from the camera) views, where the trimmed videos did not contain any of the screened artifacts. By following this process, 89 patient sets (2 sagittal and 2 coronal videos per patient) for a total of 178 sagittal videos and 178 coronal view videos were found appropriate for further analysis, out of the initial 230 patient sets.

Algorithm performance in the sagittal and coronal planes was assessed by comparing automated outputs to manual verification of the movement plane, stride detection, and movement direction. A single examiner reviewed all videos to establish the ground truth for these parameters.

Accuracy was evaluated by comparing the algorithm results to the manual EVGS scores provided in the Sanatorio del Norte dataset. These EVGS scores were assigned by experts at the Sanatorio del Norte hospital using sagittal, coronal, and overhead views to evaluate each video. The algorithm's scores were categorized into three groups: same scores, scores within a one-point difference, and scores with a difference greater than one. Accuracy for each of the 17 EVGS movements was calculated. The accuracy for each leg (right and left) was calculated separately, and the average of these two accuracies was reported for each of the 17 parameters. In this study, very high accuracy was defined as 90%-100%, high as 80%-90%, moderate as 70%-80%, and low as below 70%.

5.5 Results

For both sagittal and coronal planes, the algorithm correctly distinguished between sagittal and coronal views for all videos. Therefore, accuracy, sensitivity, specificity, and precision were 100%,

culminating in an F1-score of 1.0.

For detecting direction of motion, the sagittal view had 99.08% accuracy, 100% sensitivity, and 98.20% specificity. Precision was 98.17% and the F1-score was 0.99. In the coronal view, accuracy, sensitivity, specificity, and precision were 100%, with an F1-score of 1.0.

The algorithm had an overall stride detection rate of 95.4% (all strides detected for 104 of 109 patients sets). Two patient sets did not detect right strides, two other patient sets did not detect right and left strides, and one set did not detect left strides. The challenges experienced in these cases were attributed to constant zooming that interfered with stride-to-stride analysis because keypoint distances relative to the floor changed. These results further indicated that, while the algorithm performed very well for most cases with very high accuracy and robustness, recording condition-related factors can affect performance.

Figure 5.2 and Figure 5.3 show algorithm performance of the sagittal plane EVGS parameters, indicating how well automated scoring agreed with expert assessments. The algorithm had highly accurate sagittal parameters for peak hip flexion in swing, knee extension in swing, peak sagittal trunk position, maximum ankle dorsiflexion in stance, and peak knee flexion in swing, with accuracies between 90% and 94%.

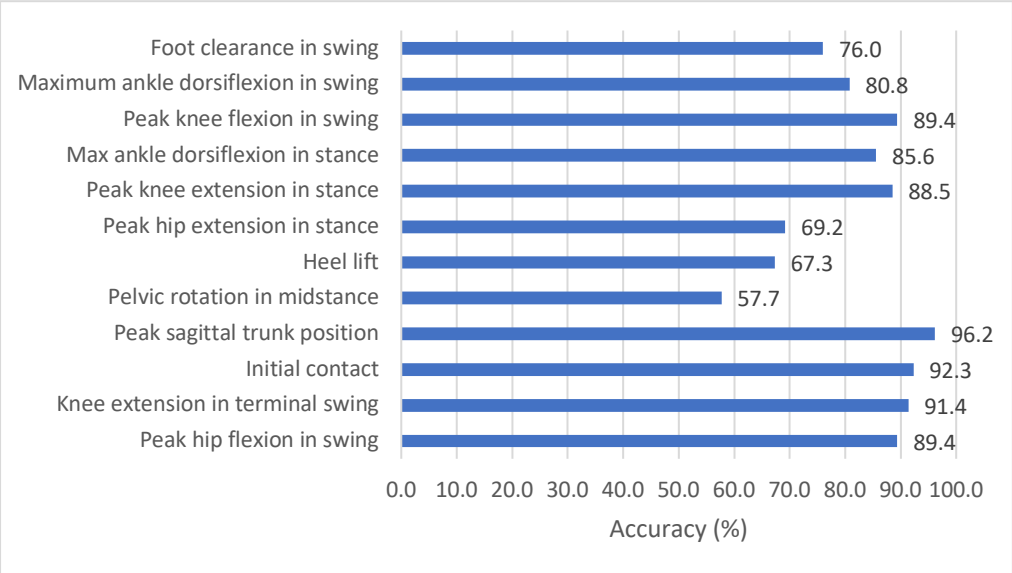

Figure 5.2 EVGS scoring accuracy for sagittal plane parameters (average of left and right legs), for results equal to ground truth

Initial contact, peak knee extension in stance, maximum ankle dorsiflexion in swing, and foot clearance in swing had slightly lower accuracy percentages, between 84% and 88%. Accuracy ranged between 70% and 76% for heel lift and peak hip extension during the stance. Pelvic rotation at midstance produced the lowest accuracy at 62%. Parameters with higher accuracy had fewer one-score deviations, reflecting better algorithm performance. Contrarily, medium and low accuracy parameters had more one-score changes.

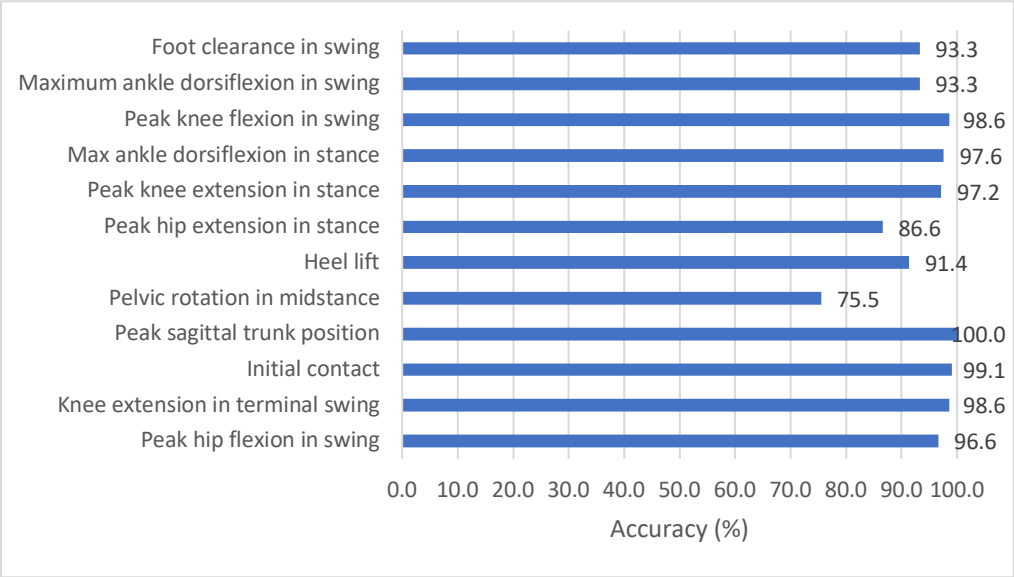

Figure 5.3 EVGS scoring accuracy for sagittal plane parameters (average of left and right legs), for results within one score from ground truth

Figure 5.4 shows EVGS scoring accuracy for coronal plane parameters, for results that were equal to ground truth (average of left and right legs). Figure 5.5 shows accuracy for results that were within 1 score from ground truth. Maximum pelvic obliquity in stance had the highest accuracy (94%), followed by knee progression angle. Maximum lateral shift of the trunk and foot rotation had moderate accuracy while hindfoot valgus/varus parameter had the lowest accuracy with 58%. Some parameters with higher accuracies had fewer one-score deviations, indicating better algorithm performance. While parameters with medium and low accuracies had more one-score changes.

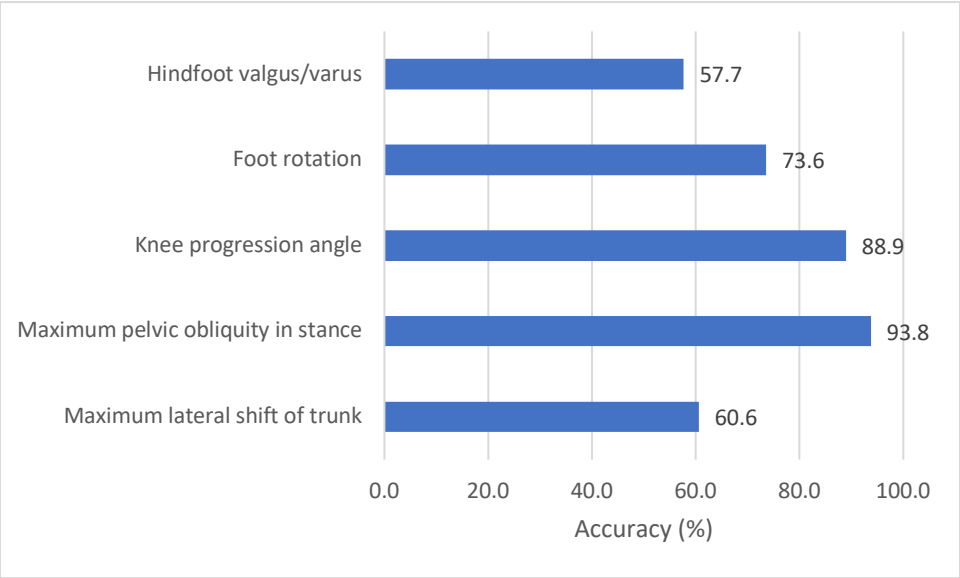

Figure 5.4 EVGS scoring accuracy for coronal plane parameters (average of left and right legs), for results equal to ground truth

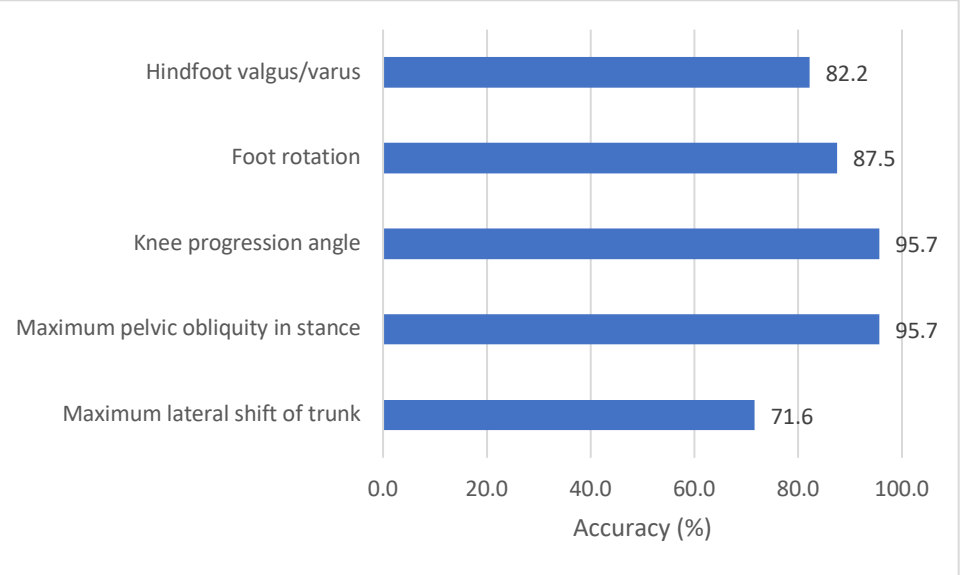

Figure 5.5 EVGS scoring accuracy for coronal plane parameters (average of left and right legs), for results within one score from ground truth

5.6 Discussion

This research demonstrated that an automated algorithm for EVGS scoring can produce appropriate results for clinical decision-making. The development process helped to define video data

collection recommendations that should help improve scoring accuracy when using this tool. Even with high accuracies for most parameters, areas for further improvements were identified.

5.6.1 Sagittal Plane Parameters

Most sagittal plane parameters had good or excellent accuracy, indicating that this is an appropriate tool for clinical assessment. The best results were observed for peak hip flexion in swing, knee extension in swing, peak sagittal trunk position, maximum ankle dorsiflexion in stance, and peak knee flexion in swing, and peak knee extension in stance, maximum ankle dorsiflexion in swing, and foot clearance in swing also showed high accuracy. These parameters used keypoints and joint angles that were well defined across video frames, which contributed to the successful results.

Heel lift and peak hip extension in stance had moderate accuracy. The heel lift score calculation depends on the foot strike and foot-off events, and this score was sensitive to small shifts of these gait events. Ramesh et al. [23] mentioned that a change of one frame results in a score change from 0 to 1. Alternative methods of scoring heel lift could be considered for future studies in which scores would be independent of the stride events and more precisely reflect the inter-limb kinematics.

For hip extension during stance, moderate results could relate to how the hip angle is defined from OpenPose keypoints. Since a pelvis segment cannot be defined using OpenPose keypoints, the hip angle represents the angle between the trunk axis (neck to mid-hip keypoints) and thigh (hip to knee keypoints). Human scorers perceive hip extension as the thigh angle relative to the pelvis. The trunk angle may differ from pelvis angle, especially in pathological gait where the trunk can be bent over and have a greater range of motion. Thus, clinician assessments can differ from the algorithm. Further advancement in AI-based pose detection models is needed to add more pelvis keypoints, to enable a separate pelvis segment for biomechanical analysis. Alternatively, if a fixed image plane can be established, then thigh angle to vertical could be considered as a surrogate measure to score hip movement parameters.

Pelvic rotation during midstance exhibited the lowest accuracy (58%); however, the inter-observer reliability for this parameter among experienced human raters was only 60% complete agreement. This lower accuracy maybe related to the lack of a distinct pelvis segment [83]. For the algorithm, the pelvic rotation angle was estimated using a line connecting the right and left hip joints in respect

to the y-axis (vertical) of the sagittal plane in the image coordinate system [23]. Other surrogate measures could be considered in future research. For example, the change of inter-hip distance in the coronal plane. Moreover, an investigation into new pose detection methods that estimate the depth axis might further improve the automated scoring of EVGS during transverse plane movements. Given the limitations in both manual and automated methods, this lower accuracy may be acceptable since the algorithm performed at a level similar to human evaluators.

5.6.2 Coronal Plane Parameters

The majority of coronal EVGS parameters had high accuracy. Parameters that were difficult to estimate in the coronal plane included maximum lateral trunk shift, foot rotation and hindfoot valgus/varus. Accuracy for maximum lateral trunk shift was relatively low (61%), and the observed inter-observer reliability among experienced human raters was only 68% complete agreement for this EVGS parameter [83]. This suggests that even trained professionals exhibit notable variability when evaluating maximum lateral trunk shift. Research has repeatedly demonstrated that, when evaluating gait impairments in children with CP, EVGS is more reliable for distal segments (foot, ankle, knee) than for proximal segments (trunk, pelvis, hip) [22], [83], [84] . This implies that some of the differences for trunk shift could be attributed to manual scoring.

Despite the relatively low accuracy (~58%) in automated scoring of hindfoot valgus/varus, the inter-observer reliability for this parameter among experienced human scorers was also modest, with only 72% complete agreement [83]. In the coronal view, heel and toe keypoints can usually be clumped, overlapped, or occluded by the big-toe keypoint. Since ankle and heel keypoints are close to each other in this plane, moving further away from the camera would reduce the distance in pixels (i.e., since the person is smaller in the camera field of view), keypoints can be easily occluded during gait and hence would contribute to discrepancies in EVGS scoring. This problem is not unique to the algorithm, since the human estimators face similar difficulties in estimating foot keypoints from such images [23]. These factors might also affect foot rotation scoring.

Excessive use of zoom during recording was also a limiting factor for assessing coronal parameters. High magnification can introduce distortion in spatial relationships, affecting the algorithm's ability to accurately evaluate parameters like hindfoot valgus/varus and lateral trunk shift. When zoom fluctuates (i.e., when the person rapidly zooms in and out), the algorithm struggles to

maintain a stable frame of reference, which is essential for precise tracking. This inconsistency not only hinders analysis of subtle lateral and rotational movements but also disrupts the person's relative position within the frame. A stable and consistent viewpoint between frames is crucial for accurately evaluating these coronal parameters since variability in zoom can obscure the subtle shifts in alignment and movement that are critical for a reliable assessment of hindfoot and trunk positioning.

5.6.1 Key Insights into Video Recording Parameters and Participant Gait Patterns for EVGS Analysis

The Sanatorio del Norte video dataset contains sagittal, coronal, and overhead views for the patients participating in EVGS analysis. Only sagittal and coronal views were used in the algorithm evaluation, since the general instructions of EVGS only include these planes. The overhead view can provide useful clinical information (especially about the pelvic rotation parameter) but is not part of the standard EVGS protocol and hence not included in our evaluation. Future versions of the algorithm may be designed to incorporate overhead views, if available, to enable more comprehensive gait analyses, particularly for parameters that are difficult to assess in sagittal and coronal planes.

Some people in the dataset used gait assistive devices like walkers and crutches. These assistive devices did not affect algorithm performance since OpenPose provided appropriate body keypoints even in the presence of walkers or crutches. This speaks to the strength of pose detection models for accommodating people with different mobility needs.

The heel lift EVGS parameter is descriptive. Specific timing and conditions are defined during the stance phase, such that "heel lift normally occurs between opposite foot level and opposite foot contact (Normal). Early heel lift indicates that heel lift precedes the opposite foot being level with the stance foot. Delayed heel lift is present if heel lift occurs with or after opposite foot contact [130]. Since these definitions are visual judgments and qualitative, they are highly dependent on the expertise of the observer and the clarity of the video. In contrast, the automated algorithm calculates heel lift in a quantitative and automated way, based on the analysis of relative positions between heel and back toe in different phases of the gait cycle. The algorithm estimates the "heel-toe angle," which is a measure to determine whether the foot is flat, lifting, or in some other

position.

However, the algorithm's effectiveness hinges on accurate detection of foot keypoints, particularly for the leg farthest from the camera. Since the leg farthest from the camera can be partially obscured or less visible, keypoint identification can be adversely affected, thereby failing to provide appropriate data to calculate and determine the gait phase.

5.6.2 Implementing Alternative Indices and Their Potential Effects on Cerebral Palsy Gait Analysis

Advantages of the EVGS include its suitability for analysis in patients with CP aged 5-40 years by evaluation of a wide range of parameters in all three anatomical planes to ensure comprehensiveness of gait pathology assessment. The higher degree of intra- and inter-rater reliability than other similar metrics, even by less experienced raters, lends strength to its use across diverse clinical settings. EVGS can also be used to track outcomes of interventions like orthoses and surgeries. Despite its advantages, there are limitations to EVGS, especially when assessing pelvic and hip movements in the frontal and transverse plane. The complexity of these movements, besides the subjective nature of visual interpretation, might lower the sensitivity for some gait abnormalities associated with CP.

Other visual gait indices could be used to complement EVGS scoring, if these were also implemented algorithmically. Adding alternative indices like G.A.I.T., SF-GT, WGS, RGVA along with EVGS could resolve shortfalls, potentially enhancing the outcomes of this research study. G.A.I.T. stands out due to its design, which accounts for known limitations of other indices by providing a detailed evaluation of coordinated movement components. G.A.I.T demonstrated high sensitivity in detecting performance evolution after therapeutic interventions. Incorporating an algorithmic implementation of G.A.I.T. could provide outcome measures for physiotherapy or exoskeleton use in CP patients, in terms of subtle improvements in coordination and quality of movement. WGS and RVGA are sensitive to alterations of gait following physical therapy and can thus complement the EVGS by focusing on different features of gait pathology, such as hemiplegic or stroke-related gait deficits.

Care should be taken to match the intended indices with the population under investigation, with

their respective scoring systems adapted to CP-specific features of gait. Ultimately, a suite of indices, underpinned by robust protocols and standardized methodologies, may enable a comprehensive evaluation of gait pathology and the outcomes of interventions in CP.

5.7 Conclusion

An automated approach for scoring EVGS was successfully used with patient data acquired in typical clinical conditions, with algorithmic performance almost comparable to expert scoring. The algorithm was excellent for detecting the plane and direction of movement in both sagittal and coronal views. Of the 17 EVGS parameters evaluated, six achieved an accuracy of 90–94%, five achieved high accuracy at 84–89%, three achieved a moderate accuracy of 70–76%, while the final three had a low accuracy of 58–62% when benchmarked against the expert assessments. These results show the promise of automation for streamlining clinical visual gait analysis so that more routine monitoring of patients can be conducted without the need for extensive clinician time. Future developments aim to address limitations related to depth perception, stability, and occlusion to enhance algorithm's performance. In order to make the system completely automated, future work should also include video quality analysis to automatically detect and focus on the patient when multiple individuals appear in the frame, and to intelligently crop the video where necessary to ensure the input is optimized for analysis.

6 Thesis Summary, Conclusions and Future work

6.1 Research Summary

Gait abnormalities affect the ability to carry out activities of daily living, thereby adversely affecting mobility, independence, and quality of life. Early detection of gait abnormalities is important since early intervention can decrease long-term effects. An accurate diagnosis, provided at an early stage, aids in determining targeted strategies for better patient outcomes. Gait analysis plays, in this aspect, a central role in the distinction between a normal and pathological gait pattern, enabling the clinician to bring important information necessary for diagnosis and treatment.

The Edinburgh Visual Gait Score has been one of the most widely used clinical tools developed for evaluating gait patterns. EVGS has a comprehensive visual assessment method that allows clinicians to grade several kinematic parameters regarding the deviations of gait. However, manual scoring can be time-consuming and might cause variability, so there is strong motivation toward automation. Automatic gait analysis through EVGS would introduce enhanced efficiency, consistency, and accessibility for both clinicians and patients. For clinicians, automation delivers convenience in decision-making because real-time, accurate, detailed gait analysis could be provided at the point of patient contact. Given this facilitation in decision-making, there is now the possibility of timely adjustments in treatment plans because it enables periodic patient monitoring. This automation also eliminates human error, including inter reviewer differences.

Automated gait analysis could reduce the logistic challenges in traditional clinical gait assessments. Gait analysis is usually performed in a special laboratory and requires the patient to travel to a specialized healthcare facility. The automated markerless approach offers a low-interference, localized solution, hence enabling gait assessment in an environment familiar and convenient for the patient. This increased accessibility opens a window for early diagnosis and management even in the most remote or under-resourced areas.

The basis of automating gait analysis with EVGS rests on three modules:

- **Pose Estimation to Detect Joints and Body Landmarks:** Pose estimation models are deep learning-based models that extract relevant body keypoints from videos without the need for physical markers, hence simplifying data acquisition.

- **Stride and Event Detection:** A stride detection module identifies gait strides and foot events. These stride parameters define the gait cycle and are required for EVGS analysis.
- **Directional and Parameter Computation:** This module determines the person's direction movement direction, which is required to calculate sagittal and coronal gait parameters.

This thesis presents new methods in stride detection and markerless visual gait analysis. The review of related literature and methodologies formed a solid foundation for developing and evaluating the thesis objectives. Detailed analyses demonstrated how stride recognition techniques, pose estimation models, and automatic EVGS evaluation could provide acceptable gait outcome measures.

Objective 1: Develop an algorithm to detect planes, strides, direction of movement and automatically determine the EVGS score from patient video data set obtained.

An algorithm to automatically calculate the EVGS scores was implemented. This thesis developed new approaches for detecting planes, direction of movement for sagittal and coronal planes, error handling for stride detection and EVGS parameter calculation. To assess the proposed algorithmic approach, stride identification, movement direction, and plane detection results were compared to manually reviewed ground truth. The algorithm had excellent results, with the few errors due to excessive camera zooming or multiple people confusion in the video.

Objective 2: Validate the algorithm on a large dataset

Accuracy in 17 parameters of EVGS ranged from 90 to 94% in six, from 84 to 89% in five, from 70 to 76% in three, and from 58 to 62% in three parameters. The algorithm had good performance for most of the EVGS parameters; however, there is still a need for improvement of parameters with low scores.

6.2 Limitations

The study included people aged from 6 to 40 years, a sample with both pediatric and adult participants. Though this population sample is useful for evaluating algorithm performance in a

general clinical environment, differences in body size, proportions, and movement dynamics between children and adults are not considered. The EVGS was originally created for pediatric subjects and targeted particularly to children with CP. Physical differences among different age groups might also not fall precisely within the parameters that EVGS have specified for pediatric gait. This may affect the generality and the accuracy of the algorithm. In the future, the algorithm could be tuned for different subgroups, such as pediatric or adult or with different ethnicities. This would require a larger data set for each subgroup.

The development and evaluation datasets were from one clinic. Future evaluations with videos from different clinical facilities are required to verify that the pose detection model and EVGS scoring algorithm provides consistent results across varying video capture environments. Note that the expectation is that the video capture best practices are followed, since poor video recording is acknowledged as a problem for any gait assessment application.

6.3 Best Practices for Video Recording

Based on experiences when conducting this thesis, some best practices in video recording for accurate automated analysis of the EVGS are suggested. First, the camera should not change zoom during recording. Of equal importance is the assurance that the whole body remains in the frame of the video during recording, to provide quality keypoints for algorithm input. Note that the person should be a minimum of 60 by 80 pixels in the video for good OpenPose keypoint detection. Therefore, the camera should be in a location where the person is more than a third of the frame height.

Similarly, a non-moving camera, aligned correctly for the plane of interest, is ideal for analysis since the only moving item is the person of interest. A tripod is highly recommended since this eliminates camera motion. Only the person under analysis should be within the frame of the video since multiple individuals within the frame distract from and complicate the automated analysis. However, since multiple people are detected by OpenPose, additional postprocessing software could be developed to provide consistently good keypoints for the person of interest (i.e., current multiple person identification is insufficient to automatically identify a consistent keypoint set for an entire video).

The environment where the recording occurs makes a big difference in the usefulness of the video.

The walkway should be clear, with no obstacles to impede or occlude the view of the person's movements.

One other important factor is the duration of the walking trial. Recording at least three strides should provide enough data to represent the person's typical gait patterns.

Following these best practices will greatly enhance the quality of video recordings and the quality of automated EVGS scoring.

6.4 Future Work

This thesis introduces an innovative approach to gait analysis that combines markerless technology with clinical-based assessment. This system could be used to remotely assess gait in a familiar and local environment, enabling better engagement between healthcare professionals and patients. The proposed system should be pragmatic, valid, affordable, and offer automated EVGS gait assessment. Future research could involve development of a smartphone app to enable appropriate video capture and automatically generate EVGS scores for participants. Such apps would facilitate gait analysis without expensive equipment and enable easy gait assessment from any location.

The current coronal detection algorithm used fixed threshold value for R_3. Given the high level of individual and environmental variation, these may not generalize well. A study in the future could investigate dynamic thresholds determined from ratios or some adaptive equations. In such a situation, the algorithm would automatically adjust thresholds, rendering the algorithm more robust and further improving accuracy. ROC and PR curves can be used to evaluate how accuracy varies with threshold

EVGS requires steady state strides for scoring. Therefore, the automated system needs to appropriately segment the video into several consecutive strides (i.e., no turns or pauses). This automated segmentation must deal with changes of direction, stepping out and back into the field of view, and disrupted tracking of the same leg.

Future improvement can be made by using smartphone sensors output (i.e., acceleration, phone orientation, etc.) to adjust body keypoints to a consistent reference frame (e.g., gravity). to enhance the accuracy of stride detection and subsequent EVGS scoring. This is more relevant when foot-

related parameters are considered.

Machine learning and alternative pose estimation models could help automate and increase the accuracy of foot event scoring and stride frame identification.

References

[1] A. Muro-de-la-Herran, B. Garcia-Zapirain, and A. Mendez-Zorrilla, "Gait Analysis Methods: An Overview of Wearable and Non-Wearable Systems, Highlighting Clinical Applications," *Sensors*, vol. 14, no. 2, pp. 3362–3394, Feb. 2014, doi: 10.3390/s140203362.

[2] F. B. Horak and M. Mancini, "Objective Biomarkers of Balance and Gait for Parkinson's Disease Using Body-Worn Sensors," *Mov. Disord. Off. J. Mov. Disord. Soc.*, vol. 28, no. 11, pp. 1544–1551, Sep. 2013, doi: 10.1002/mds.25684.

[3] M. Ghislieri, V. Agostini, L. Rizzi, M. Knaflitz, and M. Lanotte, "Atypical Gait Cycles in Parkinson's Disease," *Sensors*, vol. 21, no. 15, p. 5079, Jul. 2021, doi: 10.3390/s21155079.

[4] B. Galna, S. Lord, D. J. Burn, and L. Rochester, "Progression of Gait Dysfunction in Incident Parkinson's Disease: Impact of Medication and Phenotype," *Mov. Disord. Off. J. Mov. Disord. Soc.*, vol. 30, no. 3, pp. 359–367, Mar. 2015, doi: 10.1002/mds.26110.

[5] F. Pieruccini-Faria *et al.*, "Gait Variability Across Neurodegenerative and Cognitive Disorders: Results from the Canadian Consortium of Neurodegeneration in Aging (CCNA) and the Gait and Brain Study," *Alzheimers Dement. J. Alzheimers Assoc.*, vol. 17, no. 8, pp. 1317–1328, Aug. 2021, doi: 10.1002/alz.12298.

[6] Q. Tian *et al.*, "Association of Combined Slow Gait and Low Activity Fragmentation With Later Onset of Cognitive Impairment," *JAMA Netw. Open*, vol. 4, no. 11, p. e2135168, Nov. 2021, doi: 10.1001/jamanetworkopen.2021.35168.

[7] R. Baker, "Gait Analysis Methods in Rehabilitation," *J. Neuroengineering Rehabil.*, vol. 3, p. 4, Mar. 2006, doi: 10.1186/1743-0003-3-4.

[8] C. Rathinam, A. Bateman, J. Peirson, and J. Skinner, "Observational Gait Assessment Tools in Paediatrics – A Systematic Review," *Gait Posture*, vol. 40, no. 2, pp. 279–285, Jun. 2014, doi: 10.1016/j.gaitpost.2014.04.187.

[9] J. J. Daly *et al.*, "Development and Testing of the Gait Assessment and Intervention Tool (G.A.I.T.): A Measure of Coordinated Gait Components," *J. Neurosci. Methods*, vol. 178, no. 2, pp. 334–339, Apr. 2009, doi: 10.1016/j.jneumeth.2008.12.016.

[10] K. A. Hughes and F. Bell, "Visual Assessment of Hemiplegic Gait Following Stroke: Pilot Study," *Arch. Phys. Med. Rehabil.*, vol. 75, no. 10, pp. 1100–1107, Oct. 1994, doi: 10.1016/0003-9993(94)90085-x.

[11] S. E. Lord, P. W. Halligan, and D. T. Wade, "Visual Gait Analysis: The Development of a Clinical Assessment and Scale," *Clin. Rehabil.*, vol. 12, no. 2, pp. 107–119, Apr. 1998, doi: 10.1191/026921598666182531.

[12] M. D. Gor-García-Fogeda, R. Cano de la Cuerda, M. Carratalá Tejada, I. M. Alguacil-Diego, and F. Molina-Rueda, "Observational Gait Assessments in People With Neurological

Disorders: A Systematic Review," *Arch. Phys. Med. Rehabil.*, vol. 97, no. 1, pp. 131–140, Jan. 2016, doi: 10.1016/j.apmr.2015.07.018.

[13] U. Kharb and T. Gautam, "Review and Analysis of Various Human Pose Estimation Models," Jul. 14, 2022, *Social Science Research Network, Rochester, NY*: 4157643. doi: 10.2139/ssrn.4157643.

[14] R. Josyula and S. Ostadabbas, "A Review on Human Pose Estimation," *ArXiv*, Oct. 2021, Accessed: Jan. 28, 2025. [Online]. Available: https://www.semanticscholar.org/paper/A-Review-on-Human-Pose-Estimation-Josyula-Ostadabbas/8539dfedd833d17869340f1d89c86c6c7fb57f6b

[15] J. Janardhanan and S. Umamaheswari, "A comprehensive study on human pose estimation," in *2022 8th International Conference on Advanced Computing and Communication Systems (ICACCS)*, Mar. 2022, pp. 535–541. doi: 10.1109/ICACCS54159.2022.9784965.

[16] C. S. Tony Hii, K. B. Gan, N. Zainal, N. M. Ibrahim, S. A. Md. Rani, and N. A. Shattar, "Marker Free Gait Analysis using Pose Estimation Model," in *2022 IEEE 20th Student Conference on Research and Development (SCOReD)*, Nov. 2022, pp. 109–113. doi: 10.1109/SCOReD57082.2022.9974096.

[17] Z. Cao, G. Hidalgo, T. Simon, S.-E. Wei, and Y. Sheikh, "OpenPose: Realtime Multi-Person 2D Pose Estimation Using Part Affinity Fields," *IEEE Trans. Pattern Anal. Mach. Intell.*, vol. 43, no. 1, pp. 172–186, Jan. 2021, doi: 10.1109/TPAMI.2019.2929257.

[18] Y. Guo, J. Liu, G. Li, L. Mai, and H. Dong, "Fast and flexible human pose estimation with hyperPose," in *Proceedings of the 29th ACM International Conference on Multimedia*, Oct. 2021, pp. 3763–3766. doi: 10.1145/3474085.3478325.

[19] V. Bazarevsky, I. Grishchenko, K. Raveendran, T. Zhu, F. Zhang, and M. Grundmann, "BlazePose: On-device Real-time Body Pose tracking," Jun. 17, 2020, *arXiv*: arXiv:2006.10204. doi: 10.48550/arXiv.2006.10204.

[20] J. M. Graving *et al.*, "DeepPoseKit, A Software Toolkit for Fast and Robust Animal Pose Estimation Using Deep Learning," *eLife*, vol. 8, p. e47994, Oct. 2019, doi: 10.7554/eLife.47994.

[21] Ł. Kidziński, B. Yang, J. L. Hicks, A. Rajagopal, S. L. Delp, and M. H. Schwartz, "Deep Neural Networks Enable Quantitative Movement Analysis Using Single-Camera Videos," *Nat. Commun.*, vol. 11, no. 1, p. 4054, Aug. 2020, doi: 10.1038/s41467-020-17807-z.

[22] A. Aroojis, B. Sagade, and S. Chand, "Usability and Reliability of the Edinburgh Visual Gait Score in Children with Spastic Cerebral Palsy Using Smartphone Slow-Motion Video Technology and a Motion Analysis Application: A Pilot Study," *Indian J. Orthop.*, vol. 55, no. 4, pp. 931–938, Jan. 2021, doi: 10.1007/s43465-020-00332-y.

[23] S. H. Ramesh, E. D. Lemaire, A. Tu, K. Cheung, and N. Baddour, "Automated Implementation of the Edinburgh Visual Gait Score (EVGS) Using OpenPose and Handheld

Smartphone Video," *Sensors*, vol. 23, no. 10, Art. no. 10, Jan. 2023, doi: 10.3390/s23104839.

[24] A. Alharbi, K. Equbal, S. Ahmad, H. U. Rahman, and H. Alyami, "Human Gait Analysis and Prediction Using the Levenberg-Marquardt Method," *J. Healthc. Eng.*, vol. 2021, p. 5541255, Feb. 2021, doi: 10.1155/2021/5541255.

[25] D. J. Mayich, A. Novak, D. Vena, T. R. Daniels, and J. W. Brodsky, "Gait analysis in orthopedic foot and ankle surgery--topical review, part 1: principles and uses of gait analysis," *Foot Ankle Int.*, vol. 35, no. 1, pp. 80–90, Jan. 2014, doi: 10.1177/1071100713508394.

[26] L. M. Silva and N. Stergiou, "The basics of gait analysis," in *Biomechanics and Gait Analysis*, Elsevier, 2020, pp. 225–250. doi: 10.1016/B978-0-12-813372-9.00007-5.

[27] R. Di Gregorio and L. Vocenas, "Identification of Gait-Cycle Phases for Prosthesis Control," *Biomimetics*, vol. 6, no. 2, Art. no. 2, Jun. 2021, doi: 10.3390/biomimetics6020022.

[28] A. Leal-Junior and A. Frizera-Neto, "Gait analysis: overview, trends, and challenges☆," in *Optical Fiber Sensors for the Next Generation of Rehabilitation Robotics*, A. Leal-Junior and A. Frizera-Neto, Eds., Academic Press, 2022, pp. 53–64. doi: 10.1016/B978-0-32-385952-3.00011-1.

[29] A. Alamdari and V. N. Krovi, "Chapter Two - A Review of Computational Musculoskeletal Analysis of Human Lower Extremities," in *Human Modelling for Bio-Inspired Robotics*, J. Ueda and Y. Kurita, Eds., Academic Press, 2017, pp. 37–73. doi: 10.1016/B978-0-12-803137-7.00003-3.

[30] A. Nandy, S. Chakraborty, J. Chakraborty, and G. Venture, "1 - Introduction," in *Modern Methods for Affordable Clinical Gait Analysis*, A. Nandy, S. Chakraborty, J. Chakraborty, and G. Venture, Eds., Academic Press, 2021, pp. 1–15. doi: 10.1016/B978-0-323-85245-6.00012-6.

[31] T. A. L. Wren, G. E. Gorton, S. Ounpuu, and C. A. Tucker, "Efficacy of Clinical Gait Analysis: A Systematic Review," *Gait Posture*, vol. 34, no. 2, pp. 149–153, Jun. 2011, doi: 10.1016/j.gaitpost.2011.03.027.

[32] F. M. Chang, A. J. Seidl, K. Muthusamy, A. K. Meininger, and J. J. Carollo, "Effectiveness of Instrumented Gait Analysis in Children With Cerebral Palsy - Comparison of Outcomes," *J. Pediatr. Orthop.*, vol. 26, no. 5, p. 612, Oct. 2006, doi: 10.1097/01.bpo.0000229970.55694.5c.

[33] H. M. Horstmann and E. E. Bleck, *Orthopaedic Management in Cerebral Palsy*, 2 edition. London : United Kingdom: Mac Keith Press, 2007.

[34] K. M. Schweitzer and S. G. Parekh, "Comparison of Gait Biomechanics: Ankle Fusion Versus Ankle Replacement," *Semin. Arthroplasty*, vol. 21, no. 4, pp. 223–229, Dec. 2010, doi: 10.1053/j.sart.2010.09.003.

[35] J. B. Webster and B. J. Darter, "4 - Principles of Normal and Pathologic Gait," in *Atlas of*

Orthoses and Assistive Devices (Fifth Edition), J. B. Webster and D. P. Murphy, Eds., Philadelphia: Elsevier, 2019, pp. 49-62.e1. doi: 10.1016/B978-0-323-48323-0.00004-4.

[36] B. Toro, C. J. Nester, and P. C. Farren, "The Development and Validity of the Salford Gait Tool: An Observation-Based Clinical Gait Assessment Tool," *Arch. Phys. Med. Rehabil.*, vol. 88, no. 3, pp. 321–327, Mar. 2007, doi: 10.1016/j.apmr.2006.12.028.

[37] S. R. Hamner, A. Seth, and S. L. Delp, "Muscle Contributions to Propulsion and Support During Running," *J. Biomech.*, vol. 43, no. 14, pp. 2709–2716, Oct. 2010, doi: 10.1016/j.jbiomech.2010.06.025.

[38] A. Mengarelli, A. Gentili, A. Strazza, L. Burattini, S. Fioretti, and F. Di Nardo, "Co-Activation Patterns of Gastrocnemius and Quadriceps Femoris in Controlling the Knee Joint During Walking," *J. Electromyogr. Kinesiol.*, vol. 42, pp. 117–122, Oct. 2018, doi: 10.1016/j.jelekin.2018.07.003.

[39] K. Sasaki and R. R. Neptune, "Individual Muscle Contributions to the Axial Knee Joint Contact Force During Normal Walking," *J. Biomech.*, vol. 43, no. 14, pp. 2780–2784, Oct. 2010, doi: 10.1016/j.jbiomech.2010.06.011.

[40] K. Zhao, C. Shan, and Y. Luximon, "Contributions of Individual Muscle Forces to Hip, Knee, and Ankle Contact Forces During the Stance Phase of Running: a Model-Based Study," *Health Inf. Sci. Syst.*, vol. 10, no. 1, p. 11, Jun. 2022, doi: 10.1007/s13755-022-00177-9.

[41] V. Bazarevsky, I. Grishchenko, K. Raveendran, T. Zhu, F. Zhang, and M. Grundmann, "BlazePose: On-device Real-time Body Pose tracking," Jun. 17, 2020, *arXiv*: arXiv:2006.10204. doi: 10.48550/arXiv.2006.10204.

[42] D. A. Winter, "Overall Principle of Lower Limb Support During Stance Phase of Gait," *J. Biomech.*, vol. 13, no. 11, pp. 923–927, 1980, doi: 10.1016/0021-9290(80)90162-1.

[43] H. Sadeghi, S. Sadeghi, P. Allard, H. Labelle, and M. Duhaime, "Lower Limb Muscle Power Relationships in Bilateral Able-Bodied Gait," *Am. J. Phys. Med. Rehabil.*, vol. 80, no. 11, pp. 821–830, Nov. 2001, doi: 10.1097/00002060-200111000-00006.

[44] Z. Svoboda, M. Janura, P. Kutilek, and E. Janurova, "Relationships Between Movements of the Lower Limb Joints and the Pelvis in Open and Closed Kinematic Chains During a Gait Cycle," *J. Hum. Kinet.*, vol. 51, pp. 37–43, Jul. 2016, doi: 10.1515/hukin-2015-0168.

[45] D. Dykyj, "Anatomy of Motion," *Clin. Podiatr. Med. Surg.*, vol. 5, no. 3, pp. 477–490, Jul. 1988, doi: 10.1016/S0891-8422(23)00297-5.

[46] C. M. Kawamura, M. C. de Morais Filho, M. M. Barreto, S. K. de Paula Asa, Y. Juliano, and N. F. Novo, "Comparison Between Visual and Three-Dimensional Gait Analysis in Patients with Spastic Diplegic Cerebral Palsy," *Gait Posture*, vol. 25, no. 1, pp. 18–24, Jan. 2007, doi: 10.1016/j.gaitpost.2005.12.005.

[47] R. A. States, J. J. Krzak, Y. Salem, E. M. Godwin, A. W. Bodkin, and M. L. McMulkin,

"Instrumented Gait Analysis for Management of Gait Disorders in Children with Cerebral Palsy: A Scoping Review," *Gait Posture*, vol. 90, pp. 1–8, Oct. 2021, doi: 10.1016/j.gaitpost.2021.07.009.

[48] T. A. L. Wren, C. A. Tucker, S. A. Rethlefsen, G. E. Gorton, and S. Õunpuu, "Clinical Efficacy of Instrumented Gait Analysis: Systematic Review 2020 Update," *Gait Posture*, vol. 80, pp. 274–279, Jul. 2020, doi: 10.1016/j.gaitpost.2020.05.031.

[49] W. E. Dickens and M. F. Smith, "Validation of a Visual Gait Assessment Scale for Children with Hemiplegic Cerebral Palsy," *Gait Posture*, vol. 23, no. 1, pp. 78–82, Jan. 2006, doi: 10.1016/j.gaitpost.2004.12.002.

[50] H. S. Read, M. E. Hazlewood, S. J. Hillman, R. J. Prescott, and J. E. Robb, "Edinburgh Visual Gait Score for Use in Cerebral Palsy," *J. Pediatr. Orthop.*, vol. 23, no. 3, pp. 296–301, 2003.

[51] S. Grunt, P. J. van Kampen, M. M. van der Krogt, M.-A. Brehm, C. A. M. Doorenbosch, and J. G. Becher, "Reproducibility and Validity of Video Screen Measurements of Gait in Children with Spastic Cerebral Palsy," *Gait Posture*, vol. 31, no. 4, pp. 489–494, Apr. 2010, doi: 10.1016/j.gaitpost.2010.02.006.

[52] D. E. Krebs, J. E. Edelstein, and S. Fishman, "Reliability of Observational Kinematic Gait Analysis," *Phys. Ther.*, vol. 65, no. 7, pp. 1027–1033, Jul. 1985, doi: 10.1093/ptj/65.7.1027.

[53] K. Martin *et al.*, "Development and Reliability of An Observational Gait Analysis Tool for Children with Down Syndrome," *Pediatr. Phys. Ther. Off. Publ. Sect. Pediatr. Am. Phys. Ther. Assoc.*, vol. 21, no. 3, pp. 261–268, 2009, doi: 10.1097/PEP.0b013e3181b13bca.

[54] A. Harvey and J. W. Gorter, "Video Gait Analysis for Ambulatory Children with Cerebral Palsy: Why, When, Where and How!," *Gait Posture*, vol. 33, no. 3, pp. 501–503, Mar. 2011, doi: 10.1016/j.gaitpost.2010.11.025.

[55] L. A. Koman, J. F. Mooney, B. Smith, A. Goodman, and T. Mulvaney, "Management of Cerebral Palsy with Botulinum-A Toxin: Preliminary Investigation," *J. Pediatr. Orthop.*, vol. 13, no. 4, pp. 489–495, 1993, doi: 10.1097/01241398-199307000-00013.

[56] K. G. B. Maathuis, C. P. van der Schans, A. van Iperen, H. S. Rietman, and J. H. B. Geertzen, "Gait in Children with Cerebral Palsy: Observer Reliability of Physician Rating Scale and Edinburgh Visual Gait Analysis Interval Testing scale," *J. Pediatr. Orthop.*, vol. 25, no. 3, pp. 268–272, 2005, doi: 10.1097/01.bpo.0000151061.92850.74.

[57] C. R. Brown, S. J. Hillman, A. M. Richardson, J. L. Herman, and J. E. Robb, "Reliability and Validity of the Visual Gait Assessment Scale for Children with Hemiplegic Cerebral Palsy When Used by Experienced and Inexperienced Observers," *Gait Posture*, vol. 27, no. 4, pp. 648–652, May 2008, doi: 10.1016/j.gaitpost.2007.08.008.

[58] T. A. L. Wren, S. A. Rethlefsen, B. S. Healy, K. P. Do, S. W. Dennis, and R. M. Kay, "Reliability and Validity of Visual Assessments of Gait Using A Modified Physician Rating Scale for Crouch And Foot Contact," *J. Pediatr. Orthop.*, vol. 25, no. 5, pp. 646–650, 2005,

doi: 10.1097/01.mph.0000165139.68615.e4.

[59] R. N. Boyd and H. K. Graham, "Objective Measurement of Clinical Findings in the Use of Botulinum Toxin Type A for the Management of Children with Cerebral Palsy," *Eur. J. Neurol.*, vol. 6, no. Suppl. 4, pp. S23–S35, Nov. 1999, doi: 10.1111/j.1468-1331.1999.tb00031.x.

[60] A. H. Mackey, G. L. Lobb, S. E. Walt, and N. S. Stott, "Reliability and Validity of the Observational Gait Scale in Children with Spastic Diplegia," *Dev. Med. Child Neurol.*, vol. 45, no. 1, pp. 4–11, Jan. 2003.

[61] H. K. Graham *et al.*, "Recommendations for the Use of Botulinum Toxin Type A in the Management of Cerebral Palsy," *Gait Posture*, vol. 11, no. 1, pp. 67–79, Feb. 2000, doi: 10.1016/s0966-6362(99)00054-5.

[62] B. Van Gheluwe, K. A. Kirby, P. Roosen, and R. D. Phillips, "Reliability and Accuracy of Biomechanical Measurements of the Lower Extremities," *J. Am. Podiatr. Med. Assoc.*, vol. 92, no. 6, pp. 317–326, Jun. 2002, doi: 10.7547/87507315-92-6-317.

[63] J. Nae, M. W. Creaby, A. Cronström, and E. Ageberg, "Measurement Properties of Visual Rating of Postural Orientation Errors of the Lower Extremity - A Systematic Review and Meta-Analysis," *Phys. Ther. Sport Off. J. Assoc. Chart. Physiother. Sports Med.*, vol. 27, pp. 52–64, Sep. 2017, doi: 10.1016/j.ptsp.2017.04.003.

[64] H. L. Jarvis, C. J. Nester, R. K. Jones, A. Williams, and P. D. Bowden, "Inter-Assessor Reliability of Practice Based Biomechanical Assessment of the Foot and Ankle," *J. Foot Ankle Res.*, vol. 5, no. 1, p. 14, 2012, doi: 10.1186/1757-1146-5-14.

[65] A. A. Rodriquez *et al.*, "Gait Training Efficacy Using A Home-Based Practice Model in Chronic Hemiplegia," *Arch. Phys. Med. Rehabil.*, vol. 77, no. 8, pp. 801–805, Aug. 1996, doi: 10.1016/s0003-9993(96)90260-9.

[66] A. Guzik *et al.*, "The Paediatric Version of Wisconsin Gait Scale, Adaptation for Children with Hemiplegic Cerebral Palsy: A Prospective Observational Study," *BMC Pediatr.*, vol. 18, no. 1, p. 301, Sep. 2018, doi: 10.1186/s12887-018-1273-x.

[67] R. Wellmon, A. Degano, J. A. Rubertone, S. Campbell, and K. A. Russo, "Interrater and Intrarater Reliability and Minimal Detectable Change of the Wisconsin Gait Scale When Used to Examine Videotaped Gait in Individuals Post-Stroke," *Arch. Physiother.*, vol. 5, p. 11, 2015, doi: 10.1186/s40945-015-0011-z.

[68] X. Lu, N. Hu, S. Deng, J. Li, S. Qi, and S. Bi, "The Reliability, Validity and Correlation of Two Observational Gait Scales Assessed by Video Tape for Chinese Subjects with Hemiplegia," *J. Phys. Ther. Sci.*, vol. 27, no. 12, pp. 3717–3721, Dec. 2015, doi: 10.1589/jpts.27.3717.

[69] A. Yaliman, N. Kesiktas, M. Ozkaya, N. Eskiyurt, O. Erkan, and E. Yilmaz, "Evaluation of Intrarater and Interrater Reliability of the Wisconsin Gait Scale with Using the Video Taped

Stroke Patients in A Turkish Sample," *NeuroRehabilitation*, vol. 34, no. 2, pp. 253–258, 2014, doi: 10.3233/NRE-131033.

[70] K. N. Arya, S. Pandian, V. Kumar, G. G. Agarwal, and A. Asthana, "Post-stroke Visual Gait Measure for Developing Countries: A Reliability and Validity Study," *Neurol. India*, vol. 67, no. 4, pp. 1033–1040, 2019, doi: 10.4103/0028-3886.266273.

[71] J. Bernhardt, P. J. Bate, and T. A. Matyas, "Accuracy of Observational Kinematic Assessment of Upper-Limb Movements," *Phys. Ther.*, vol. 78, no. 3, pp. 259–270, Mar. 1998, doi: 10.1093/ptj/78.3.259.

[72] S. Taş, S. Güneri, B. Kaymak, and Z. Erden, "A Comparison of Results of 3-Dimensional Gait Analysis and Observational Gait Analysis in Patients with Knee Osteoarthritis," *Acta Orthop. Traumatol. Turc.*, vol. 49, no. 2, pp. 151–159, 2015, doi: 10.3944/AOTT.2015.14.0158.

[73] P. A. Araújo, R. N. Kirkwood, and E. M. Figueiredo, "Validity and Intra- and Inter-Rater Reliability of the Observational Gait Scale for Children with Spastic Cerebral Palsy," *Braz. J. Phys. Ther.*, vol. 13, pp. 267–273, Jun. 2009, doi: https://doi.org/10.1590/S1413-35552009005000033.

[74] D. T. Kephart, S. R. Laing, A. Bagley, J. R. Davids, and V. A. Kulkarni, "Gait Analysis at Your Fingertips: Accuracy and Reliability of Mobile App Enhanced Observational Gait Analysis in Children with Cerebral Palsy," *J. Pediatr. Orthop. Soc. N. Am.*, vol. 2, no. 1, p. 94, May 2020, doi: 10.55275/JPOSNA-2020-94.

[75] "Observational Gait Analysis." Accessed: Jan. 20, 2025. [Online]. Available: https://ouhsc.edu/bserdac/dthompso/web/gait/knmatics/oga.htm

[76] B. Toro, C. J. Nester, and P. C. Farren, "The Development and Validity of the Salford Gait Tool: An Observation-Based Clinical Gait Assessment Tool," *Arch. Phys. Med. Rehabil.*, vol. 88, no. 3, pp. 321–327, Mar. 2007, doi: 10.1016/j.apmr.2006.12.028.

[77] B. Toro, C. J. Nester, and P. C. Farren, "Inter- and Intraobserver Repeatability of the Salford Gait Tool: An Observation-Based Clinical Gait Assessment Tool," *Arch. Phys. Med. Rehabil.*, vol. 88, no. 3, pp. 328–332, Mar. 2007, doi: 10.1016/j.apmr.2006.12.030.

[78] J. J. Daly, J. P. McCabe, M. D. Gor-García-Fogeda, and J. C. Nethery, "Update on an Observational, Clinically Useful Gait Coordination Measure: The Gait Assessment and Intervention Tool (G.A.I.T.)," *Brain Sci.*, vol. 12, no. 8, p. 1104, Aug. 2022, doi: 10.3390/brainsci12081104.

[79] J. Zimbelman, J. J. Daly, K. L. Roenigk, K. Butler, R. Burdsall, and J. P. Holcomb, "Capability of 2 Gait Measures for Detecting Response to Gait Training in Stroke Survivors: Gait Assessment and Intervention Tool and the Tinetti Gait Scale," *Arch. Phys. Med. Rehabil.*, vol. 93, no. 1, pp. 129–136, Jan. 2012, doi: 10.1016/j.apmr.2011.08.011.

[80] D. Raab *et al.*, "A Novel Multiple-Cue Observational Clinical Scale for Functional Evaluation

of Gait After Stroke - The Stroke Mobility Score (SMS)," *Med. Sci. Monit. Int. Med. J. Exp. Clin. Res.*, vol. 26, p. e923147, Sep. 2020, doi: 10.12659/MSM.923147.

[81] G. Hale, "EVGS Reference Guide," 2019.

[82] L. W. Robinson, N. D. Clement, J. Herman, and M. S. Gaston, "The Edinburgh visual gait score – The minimal clinically important difference," *Gait Posture*, vol. 53, pp. 25–28, Mar. 2017, doi: 10.1016/j.gaitpost.2016.12.030.

[83] A. M. L. Ong, S. J. Hillman, and J. E. Robb, "Reliability and Validity of the Edinburgh Visual Gait Score for Cerebral Palsy When Used by Inexperienced Observers," *Gait Posture*, vol. 28, no. 2, pp. 323–326, Aug. 2008, doi: 10.1016/j.gaitpost.2008.01.008.

[84] M. Del Pilar Duque Orozco *et al.*, "Reliability and Validity of Edinburgh Visual Gait Score as An Evaluation Tool for Children with Cerebral Palsy," *Gait Posture*, vol. 49, pp. 14–18, Sep. 2016, doi: 10.1016/j.gaitpost.2016.06.017.

[85] E. Viehweger *et al.*, "Influence of Clinical and Gait Analysis Experience on Reliability of Observational Gait Analysis (Edinburgh Gait Score Reliability)," *Ann. Phys. Rehabil. Med.*, vol. 53, no. 9, pp. 535–546, Nov. 2010, doi: 10.1016/j.rehab.2010.09.002.

[86] G. P. Bella, N. B. B. Rodrigues, P. J. Valenciano, L. M. A. E. Silva, and R. C. T. Souza, "Correlation Among the Visual Gait Assessment Scale, Edinburgh Visual Gait Scale and Observational Gait Scale in Children with Spastic Diplegic Cerebral Palsy," *Rev. Bras. Fisioter. Sao Carlos Sao Paulo Braz.*, vol. 16, no. 2, pp. 134–140, Apr. 2012.

[87] E. Viehweger, M. Hélix, M. Jacquemier, D. Scavarda, M. A. Rohon, and S. Scorsone-Pagny, "Application of The Edinburgh Visual Gait Score: Interobserver & Intraobserver Reliability," *Orthop. Proc.*, vol. 87-B, no. SUPP_I, pp. 69–69, Mar. 2005, doi: 10.1302/0301-620x.87bsupp_i.0870069.

[88] S. B. Gonçalves, S. B. C. Lama, and M. T. da Silva, "Three Decades of Gait Index Development: A Comparative Review of Clinical and Research Gait Indices," *Clin. Biomech. Bristol Avon*, vol. 96, p. 105682, Jun. 2022, doi: 10.1016/j.clinbiomech.2022.105682.

[89] A. Guzik and M. Drużbicki, "Application of the Gait Deviation Index in the Analysis of Post-Stroke Hemiparetic Gait," *J. Biomech.*, vol. 99, p. 109575, Jan. 2020, doi: 10.1016/j.jbiomech.2019.109575.

[90] N. Turani, A. Kemiksizoğlu, M. Karataş, and R. Ozker, "Assessment of Hemiplegic Gait Using the Wisconsin Gait Scale," *Scand. J. Caring Sci.*, vol. 18, no. 1, pp. 103–108, Mar. 2004, doi: 10.1111/j.1471-6712.2004.00262.x.

[91] M. D. Gor-García-Fogeda, R. Cano-de-la-Cuerda, J. J. Daly, and F. Molina-Rueda, "Construct Validity of the Gait Assessment and Intervention Tool (GAIT) in People With Multiple Sclerosis," *PM&R*, vol. 13, no. 3, pp. 307–313, 2021, doi: 10.1002/pmrj.12423.

[92] S. B. Gonçalves, S. B. C. Lama, and M. T. da Silva, "Three Decades of Gait Index

Development: A Comparative Review of Clinical and Research Gait Indices," *Clin. Biomech. Bristol Avon*, vol. 96, p. 105682, Jun. 2022, doi: 10.1016/j.clinbiomech.2022.105682.

[93] P. M. Chern and M. L. Leow, "P 066 - Outcomes of Botulinum Toxin Injection and the Feasibility of Using ICF-CY in Determining Botulinum Toxin Injection Therapy's Goals in Malaysia," *Gait Posture*, vol. 65, pp. 342–343, Sep. 2018, doi: 10.1016/j.gaitpost.2018.06.218.

[94] A. Cretual, K. Bervet, and L. Ballaz, "Gillette Gait Index in adults," *Gait Posture*, vol. 32, no. 3, pp. 307–310, Jul. 2010, doi: 10.1016/j.gaitpost.2010.05.015.

[95] S. Gupta and K. Raja, "Responsiveness of Edinburgh Visual Gait Score to Orthopedic Surgical Intervention of the Lower Limbs in Children with Cerebral Palsy," *Am. J. Phys. Med. Rehabil.*, vol. 91, no. 9, p. 761, Sep. 2012, doi: 10.1097/PHM.0b013e31825f1c4d.

[96] P. E. M. van Schie, R. J. Vermeulen, W. J. R. van Ouwerkerk, G. Kwakkel, and J. G. Becher, "Selective dorsal rhizotomy in cerebral palsy to improve functional abilities: evaluation of criteria for selection," *Childs Nerv. Syst. ChNS Off. J. Int. Soc. Pediatr. Neurosurg.*, vol. 21, no. 6, pp. 451–457, Jun. 2005, doi: 10.1007/s00381-004-1105-1.

[97] M. E. Eastlack, J. Arvidson, L. Snyder-Mackler, J. V. Danoff, and C. L. McGarvey, "Interrater reliability of videotaped observational gait-analysis assessments," *Phys. Ther.*, vol. 71, no. 6, pp. 465–472, Jun. 1991, doi: 10.1093/ptj/71.6.465.

[98] V. A. Kulkarni, D. T. Kephart, R. Olleac, and J. R. Davids, "Enhancing Observational Gait Analysis – Techniques and Tips for Analyzing Gait Without a Gait Lab," *J. Pediatr. Orthop. Soc. N. Am.*, vol. 2, no. 3, p. 135, Nov. 2020, doi: 10.55275/JPOSNA-2020-135.

[99] S. Borel, P. Schneider, and C. J. Newman, "Video analysis software increases the interrater reliability of video gait assessments in children with cerebral palsy," *Gait Posture*, vol. 33, no. 4, pp. 727–729, Apr. 2011, doi: 10.1016/j.gaitpost.2011.02.012.

[100] H. Abe, S. Koyanagi, Y. Kusumoto, and N. Himuro, "Intra-rater and inter-rater reliability, minimal detectable change, and construct validity of the Edinburgh Visual Gait Score in children with cerebral palsy," *Gait Posture*, vol. 94, pp. 119–123, May 2022, doi: 10.1016/j.gaitpost.2022.03.004.

[101] J. Lambrecht and L. Kästner, "Towards the usage of synthetic data for marker-less pose estimation of articulated robots in RGB images," in *2019 19th International Conference on Advanced Robotics (ICAR)*, Dec. 2019, pp. 240–247. doi: 10.1109/ICAR46387.2019.8981600.

[102] T. Nöll, A. Pagani, and D. Stricker, "Markerless Camera Pose Estimation - An Overview," in *Visualization of Large and Unstructured Data Sets - Applications in Geospatial Planning, Modeling and Engineering (IRTG 1131 Workshop)*, A. Middel, I. Scheler, and H. Hagen, Eds., in Open Access Series in Informatics (OASIcs), vol. 19. Dagstuhl, Germany: Schloss Dagstuhl – Leibniz-Zentrum für Informatik, 2011, pp. 45–54. doi: 10.4230/OASIcs.VLUDS.2010.45.

[103] A. Avogaro, F. Cunico, B. Rosenhahn, and F. Setti, “Markerless human pose estimation for biomedical applications: a survey,” *Front. Comput. Sci.*, vol. 5, Jul. 2023, doi: 10.3389/fcomp.2023.1153160.

[104] A. A. El-Sallam and A. S. Mian, “Human Body Pose Estimation from Still Images and Video Frames,” in *Image Analysis and Recognition*, A. Campilho and M. Kamel, Eds., Berlin, Heidelberg: Springer, 2010, pp. 176–188. doi: 10.1007/978-3-642-13772-3_19.

[105] M. Trumble, A. Gilbert, A. Hilton, and J. Collomosse, “Deep convolutional networks for marker-less human pose estimation from multiple views,” in *Proceedings of the 13th European Conference on Visual Media Production (CVMP 2016)*, London United Kingdom: ACM, Dec. 2016, pp. 1–9. doi: 10.1145/2998559.2998565.

[106] Y. Huang *et al.*, “Towards accurate marker-less human shape and pose estimation over time,” in *2017 International Conference on 3D Vision (3DV)*, Oct. 2017, pp. 421–430. doi: 10.1109/3DV.2017.00055.

[107] D. Grest, J. Woetzel, and R. Koch, “Nonlinear Body Pose Estimation from Depth Images,” in *Pattern Recognition*, W. G. Kropatsch, R. Sablatnig, and A. Hanbury, Eds., Berlin, Heidelberg: Springer, 2005, pp. 285–292. doi: 10.1007/11550518_36.

[108] R. Li, “The comparison of top-down and bottom-up methods in multi-person pose estimation,” *Appl. Comput. Eng.*, vol. 13, no. 1, pp. 177–182, 2023, doi: 10.54254/2755-2721/13/20230728.

[109] D. Periquito, J. C. Nascimento, A. Bernardino, and J. Sequeira, “Single Camera Hand Pose Estimation from Bottom-Up and Top-Down Processes,” in *Computer Vision, Imaging and Computer Graphics -- Theory and Applications*, S. Battiato, S. Coquillart, R. S. Laramee, A. Kerren, and J. Braz, Eds., Berlin, Heidelberg: Springer, 2014, pp. 212–227. doi: 10.1007/978-3-662-44911-0_14.

[110] M. Li, Z. Zhou, J. Li, and X. Liu, “Bottom-up pose estimation of multiple person with bounding box constraint,” in *2018 24th International Conference on Pattern Recognition (ICPR)*, Aug. 2018, pp. 115–120. doi: 10.1109/ICPR.2018.8546194.

[111] S. Sen, S. Maheshwari, and A. Kumar, “Review of Recent Developments in Human Pose Estimation,” Apr. 25, 2021, *Social Science Research Network, Rochester, NY*: 3833854. doi: 10.2139/ssrn.3833854.

[112] T. D. Nguyen and M. Kresovic, “A survey of top-down approaches for human pose estimation,” Feb. 05, 2022, *arXiv*: arXiv:2202.02656. doi: 10.48550/arXiv.2202.02656.

[113] K. Khan, R. U. Khan, R. Leonardi, P. Migliorati, and S. Benini, “Head pose estimation: A survey of the last ten years,” *Signal Process. Image Commun.*, vol. 99, p. 116479, Nov. 2021, doi: 10.1016/j.image.2021.116479.

[114] S. Mroz *et al.*, “Comparing the quality of human pose estimation with BlazePose or OpenPose,” in *2021 4th International Conference on Bio-Engineering for Smart*

Technologies (BioSMART), Dec. 2021, pp. 1–4. doi: 10.1109/BioSMART54244.2021.9677850.

[115] A. Akshay, T. Sai Varun, D. Yesvanthraja, and S. Nithyapriya, "Comparative study on pose estimators such as MoveNet Lighting, MoveNet Thunder, and OpenPose (MobileNet) model for Human Pose Estimation over Real-Time Feed – IJSREM." Accessed: Jan. 19, 2025. [Online]. Available: https://ijsrem.com/download/comparative-study-on-pose-estimators-such-as-movenet-lighting-movenet-thunder-and-openpose-mobilenet-model-for-human-pose-estimation-over-real-time-feed/

[116] E. P. Washabaugh, T. A. Shanmugam, R. Ranganathan, and C. Krishnan, "Comparing the accuracy of open-source pose estimation methods for measuring gait kinematics," *Gait Posture*, vol. 97, pp. 188–195, Sep. 2022, doi: 10.1016/j.gaitpost.2022.08.008.

[117] J. BeomJun and K. SeongKi, "Comparative Analysis of OpenPose, PoseNet, and MoveNet Models for Pose Estimation in Mobile Devices | IIETA." Accessed: Jan. 19, 2025. [Online]. Available: https://www.iieta.org/journals/ts/paper/10.18280/ts.390111

[118] M. Paci, G. Mini, M. Marchettini, and F. Ferrarello, "The Salford Gait Tool: Does the clinical experience of the raters influence the inter-rater reliability?," *Dev. Neurorehabilitation*, vol. 21, no. 2, pp. 131–132, Feb. 2018, doi: 10.1080/17518423.2016.1247922.

[119] A. H. Myriam, G. Salim, E. David, and K. Mohammad, "An automated method for analysis of gait data to aid clinical interpretation," in *2011 1st Middle East Conference on Biomedical Engineering*, Feb. 2011, pp. 119–121. doi: 10.1109/MECBME.2011.5752079.

[120] A. Viswakumar, V. Rajagopalan, T. Ray, and C. Parimi, "Human gait analysis using OpenPose," in *2019 Fifth International Conference on Image Information Processing (ICIIP)*, Nov. 2019, pp. 310–314. doi: 10.1109/ICIIP47207.2019.8985781.

[121] S. Armand, G. Decoulon, and A. Bonnefoy-Mazure, "Gait analysis in children with cerebral palsy," *EFORT Open Rev.*, vol. 1, no. 12, pp. 448–460, Dec. 2016, doi: 10.1302/2058-5241.1.000052.

[122] A. A. Hulleck, D. Menoth Mohan, N. Abdallah, M. El Rich, and K. Khalaf, "Present and future of gait assessment in clinical practice: Towards the application of novel trends and technologies," *Front. Med. Technol.*, vol. 4, p. 901331, Dec. 2022, doi: 10.3389/fmedt.2022.901331.

[123] M. R. Folle and A. P. Tedesco, "Correlation between visual gait analysis and functional aspects in cerebral palsy," *Acta Ortop. Bras.*, vol. 24, no. 5, pp. 259–261, 2016, doi: 10.1590/1413-785220162405162986.

[124] C. Sardoğan, R. Muammer, N. E. Akalan, R. Sert, and F. Bilgili, "Determining the relationship between the impairment of selective voluntary motor control and gait deviations in children with cerebral palsy using simple video-based analyses," *Gait Posture*, vol. 90, pp. 295–300, Oct. 2021, doi: 10.1016/j.gaitpost.2021.08.019.

[125] T. Tzikalagia and G. Ramdharry, “Using the Edinburgh Visual Gait Score to assess gait in children with cerebral palsy: A feasibility evaluation,” *Int. J. Ther. Rehabil.*, vol. 24, no. 10, pp. 419–426, Oct. 2017, doi: 10.12968/ijtr.2017.24.10.419.

[126] E. D’Antonio, J. Taborri, E. Palermo, S. Rossi, and F. Patanè, “A markerless system for gait analysis based on OpenPose library,” in *2020 IEEE International Instrumentation and Measurement Technology Conference (I2MTC)*, May 2020, pp. 1–6. doi: 10.1109/I2MTC43012.2020.9128918.

[127] F. Zhang *et al.*, “Comparison of OpenPose and HyperPose artificial intelligence models for analysis of hand-held smartphone videos,” in *2021 IEEE International Symposium on Medical Measurements and Applications (MeMeA)*, Jun. 2021, pp. 1–6. doi: 10.1109/MeMeA52024.2021.9478740.

[128] C. J. C. McGuirk, N. Baddour, and E. D. Lemaire, “Video-Based Deep Learning Approach for 3D Human Movement Analysis in Institutional Hallways: A Smart Hallway,” *Computation*, vol. 9, no. 12, p. 130, Dec. 2021, doi: 10.3390/computation9120130.

[129] J. A. Zeni, J. G. Richards, and J. S. Higginson, “Two simple methods for determining gait events during treadmill and overground walking using kinematic data,” *Gait Posture*, vol. 27, no. 4, pp. 710–714, May 2008, doi: 10.1016/j.gaitpost.2007.07.007.

[130] “Using The Edinburgh Gait Score PDF | PDF | Foot | Anatomical Terms Of Motion,” Scribd. Accessed: Feb. 05, 2025. [Online]. Available: https://www.scribd.com/document/326520687/Using-the-Edinburgh-Gait-Score-pdf